Electronic Supporting Information

Sub-millibar pressure gradient along a gravity-driven percolated CO_2 gas diffusion electrode for vertical scale-up

Industrial Chemistry & Materials
Submitted December 2025
Accepted Febuary 2026

Craig Armstrong,[a] Bjørnar Sandnes [b] and Enrico Andreoli [*a]

† Additional experimental information and results are provided here in support of the manuscript.

[a.] *SUSTAIN – Future Steel Manufacturing Research Hub, Department of Chemical Engineering, Faculty of Science and Engineering, Swansea University, Swansea, SA1 8EN, UK.*
[b.] *Complex Fluids Research Group, Department of Chemical Engineering, Faculty of Science and Engineering, Swansea University, Swansea, SA1 8EN, UK.*
* Corresponding author: e.andreoli@swansea.ac.uk.

Supplementary theory 3
Theoretical treatment of head losses 3
Practical methodology for calculation of head losses 4
Electrolyser platform 5
Experimental cell designs 7
Weir reservoirs 7
40 x 5 cm^2 Hele-Shaw cell 8
3.16 x 3.16 cm^2 electrolysis cell 9
32 x 1 cm^2 falling-film electrolyser 12
Electrolyte and gas circulation 14
40 x 5 cm^2 Hele-Shaw cell 14
3.16 x 3.16 cm^2 electrolysis cell 15
32 x 1 cm^2 falling-film electrolyser 18
Pressure measurements 19
Gas diffusion electrode characterisation 27
preparation 27
Scanning electron microscopy 29
Sigracet 28BC GDL 29
Freudenberg H15C13 GDL 30
Sigracet 28BC-Ag GDE 31

Freudenberg H15C13-Ag GDE....32
Water contact angle....33
Electrochemistry....34
Electrochemical impedance spectroscopy....34
Electrolysis: galvanostatic with falling film electrolyte....35
Electrolysis: galvanostatic with pumped electrolyte....41
Gas chromatograph calibration....44
Manuscript glossary....46
Abbreviations....46
Symbols....46

Supplementary theory

Theoretical treatment of head losses

In the manuscript, head losses are neglected in the theoretical interpretation for simplicity. Here, a treatment is provided for completeness.

Darcy's Law relates the flow rate Q to head gradient dh/dz as:

$$Q = -A\frac{\rho g k}{\mu}\frac{dh}{dz} = A\frac{\rho g k}{\mu}\frac{\Delta h}{L}$$

where A is the cross-sectional area, ρ and μ are the fluid density and viscosity, respectively, and k is the percolator permeability. The head gradient $\Delta h/L$ is defined here as the change in head $\Delta h \equiv h_\mathrm{t} - h_\mathrm{b}$ over length L, and is defined positive for downward flow.

In real systems, viscous head losses occur in the external electrolyser architecture (tubes, fittings), so the head at the percolator inlet and outlet are not necessarily equal to the elevations of the associated feed and drain reservoirs. Let the total head loss from feed reservoir to the top of the percolator be $\Delta h_{\mathrm{l(f\to t)}}$:

$$h_\mathrm{t} = h_\mathrm{f} - \Delta h_{\mathrm{l(f\to t)}}.$$

Similarly, flow from the base of the percolator to the drain reservoir may cause a head loss such that

$$h_\mathrm{d} = h_\mathrm{b} - \Delta h_{\mathrm{l(b\to d)}} \Rightarrow h_\mathrm{b} = h_\mathrm{d} + \Delta h_{\mathrm{l(b\to d)}}.$$

The internal percolator head drop is therefore:

$$\Delta h = h_\mathrm{t} - h_\mathrm{b} = \left(h_\mathrm{f} - \Delta h_{\mathrm{l(f\to t)}}\right) - \left(h_\mathrm{d} + \Delta h_{\mathrm{l(b\to d)}}\right) = \Delta z_{\mathrm{Res}} - \Delta h_{\mathrm{l(f\to t)}} - \Delta h_{\mathrm{l(b\to d)}}$$

where $\Delta z_{\mathrm{Res}} = z_\mathrm{f} - z_\mathrm{d}$, and we have used $h_\mathrm{f} = z_\mathrm{f}$, $h_\mathrm{d} = z_\mathrm{d}$ for free-surface heads (neglecting velocity heads).

The critical flow rate: $Q_\mathrm{c} = AK$, where K is the hydraulic conductivity, produces a constant pressure profile within the percolator corresponding to $\Delta h = L$. To compensate for parasitic losses, the reservoir separation distance must satisfy:

$$\Delta z_{\mathrm{Res}} = L + \Delta h_{\mathrm{l(f\to t)}} + \Delta h_{\mathrm{l(b\to d)}}$$

In practice, this is achieved by raising the feed reservoir by an elevation equivalent to $\Delta h_{\mathrm{l(f\to t)}}$ and lowering the drain reservoir by $\Delta h_{\mathrm{l(b\to d)}}$, restoring the idealised flat pressure profile and the intended percolator operating pressure.

Practical methodology for calculation of head losses

The head losses in the feed and drain lines of a FFE design can be estimated using the following approach.
For straight tubing, the Darcy-Weisbach equation gives the pressure loss per unit length:

$$\frac{\Delta P_{\text{tube}}}{L_{\text{tube}}} = \frac{f\rho\langle v\rangle^2}{2D_{\text{H}}}$$

where f is the Darcy friction factor which depends on the Reynolds number of the flow. ρ is the fluid density, $\langle v\rangle$ is the mean flow velocity and D_{H} is the hydraulic diameter. For a circular tube, $D_{\text{H}} = D_{\text{c}}$ (internal diameter), and the mean velocity is $\langle v\rangle = 4Q/\pi D_{\text{c}}^2$. Substituting into $\Delta P = \rho g \Delta h$ gives:

$$\Delta h_{\text{tube}} = \frac{8L_{\text{tube}} f Q^2}{\pi^2 g D_{\text{c}}^5}$$

If fittings, valves and bends are present, each introduces an additional minor loss characterised by a dimensionless coefficient K_{i}. The head loss from a single fitting is:

$$\Delta h_{\text{minor,i}} = K_{\text{i}} \frac{\langle v\rangle^2}{2g}$$

The total head loss in a line is then:

$$\Delta h_{\text{L}} = \frac{Q^2}{2gA_{\text{c}}^2}\left(\frac{fL_{\text{tube}}}{D_{\text{c}}} + \sum K_{\text{i}}\right)$$

Where $A_c = \pi D_{\text{c}}^2/4$.
Alternatively, the minor losses can be included as an equivalent length:

$$L_{\text{eq}} = L_{\text{tube}} + \frac{D_{\text{c}}}{f}\sum K_{\text{i}}$$

And used in the straight tube formula:

$$\Delta h_{\text{L}} = \frac{8L_{\text{eq}} f Q^2}{\pi^2 g D_{\text{c}}^5}$$

Published tables of K_{i} for standard fittings, elbows, and valves, allow $\Delta h_{\text{l(f}\rightarrow\text{t)}}$ and $\Delta h_{\text{l(b}\rightarrow\text{d)}}$ to be estimated directly for the head-loss balance above. In the present work additional empirical adjustments beyond the estimated head losses given here were required to eliminate pressure gradients.

Electrolyser platform

To conduct a range of experiments with gravity-fed electrolytes, a custom and bespoke electrolyser platform was built and is shown illustratively in Fig. S 1. The platform was designed to be mobile and adaptable using extruded aluminium profile beams (KJN Aluminium Profile, UK) and custom laser-cut platforms for mounting all instruments, reservoirs, and gas/liquid connections. The platform was primarily designed for conducting small scale electrolysis experiments using the 3.16 x 3.16 cm^2 chambered cell and a gravity-driven flow for GDE stability (as shown in Fig. S 1), however it was modified as needed for a range of experiments including the use of the Hele-Shaw cell and the 32 x 1 cm^2 falling-film cell as in the manuscript. For reliable electrolyte circulation under gravity, custom reservoirs featuring top and bottom tubing connections were designed and constructed from acrylic (Fig. S 2). All connection fittings were either stainless steel (Swagelok) or polypropylene (Masterflex), whereas all tubing was composed of perfluoroalkoxy alkane (Masterflex). All digital gas and liquid instruments were supplied by Alicat Scientific. The flow of gas and electrolytes through the electrolyser platform are summarised in the illustrative diagrams in Fig. S 9 and Fig. S 10 respectively.

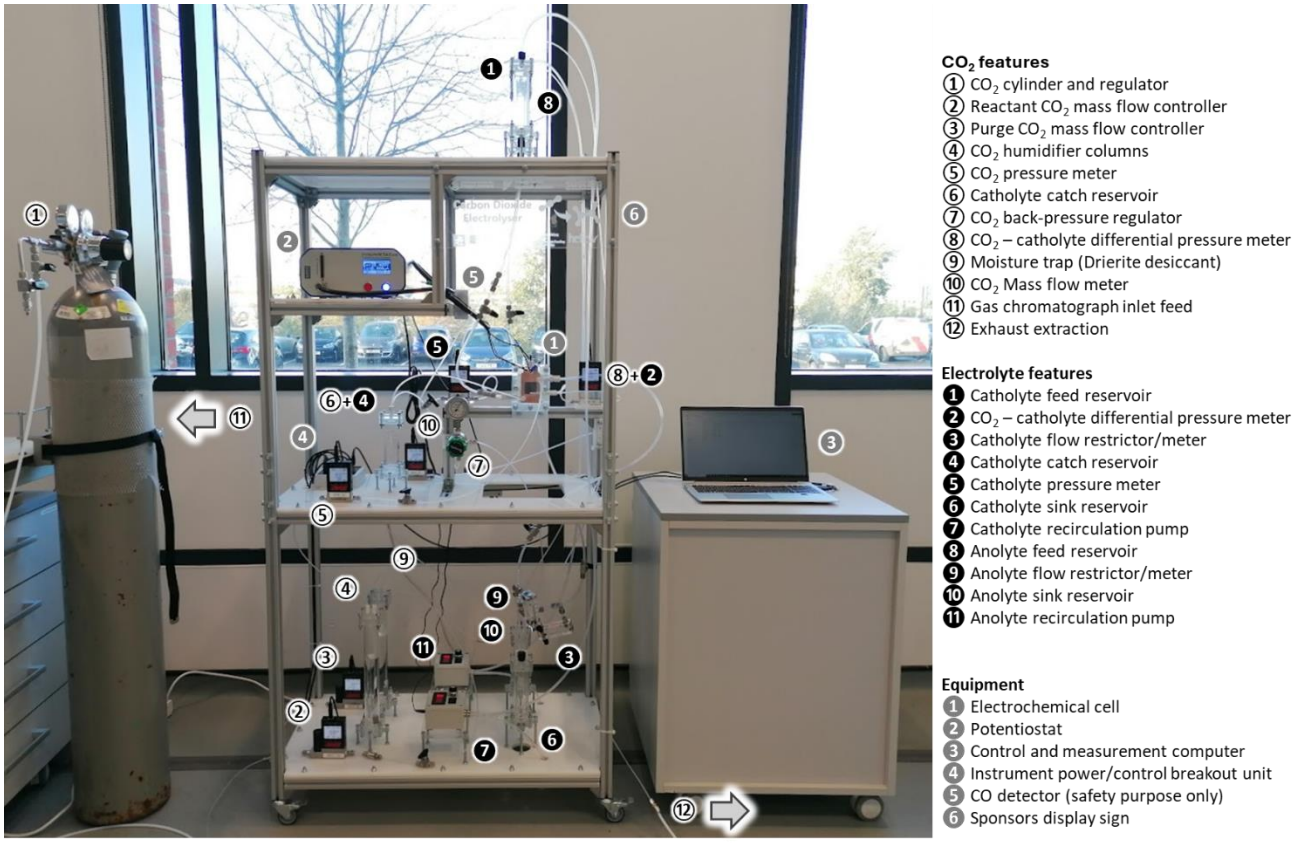

Fig. S 1 Illustrative diagram of the gravity-fed electrolyser platform. The 3.16 x 3.16 cm^2 electrolysis cell employed for threshold pressure experiments is shown (1).

To enable unimpeded flow under gravity, custom electrolyte reservoirs (❶, ❽, ❻ and ❿ in Fig. S 1) were designed as shown in Fig. S 2. These reservoirs were constructed from acrylic tube (internal diameter of 35 mm) and laser-cut acrylic flanges that were bonded by use of Tensol-12 solvent adhesive. 2 mm silicone gaskets were used to ensure a gas- and liquid-tight seal. The reservoirs feature tube fittings on their tops and bottoms for electrolyte to flow directly downwards under gravity without upwards tubing loops being required, such as when using a standard laboratory glass bottle. Additional tubing connections on the top of each reservoir linked the headspaces of the upper and lower electrolyte reservoirs such that during operation, the headspace pressures could be equalised. These pressure equalisation connections allowed electrolyte to fall under gravity unimpeded by replacing electrolyte with gas, whilst still maintaining a fully closed system. These reservoirs held an internal volume of approximately 160 mL each, however larger reservoirs with analogous construction were used where necessary (internal diameter of 60 mm and approximate volume of 700 mL) in some experiments. Similar reservoirs of height 30 cm were used to humidify the reactant and purge CO_2 feeds before reaching the electrolyser (④ in Fig. S 1). These humidification

columns were filled with ultrapure water (18.2 MΩ cm, Merck Milli-Q) and a chromatography porous filter (Thermo Scientific) was used as a bubbler. An additional reservoir (⑥ and ❹ in Fig. S 1) was used to catch catholyte upon electrode failure, for the purpose of protecting the gas instruments and the back-pressure regulator from electrolyte flooding.

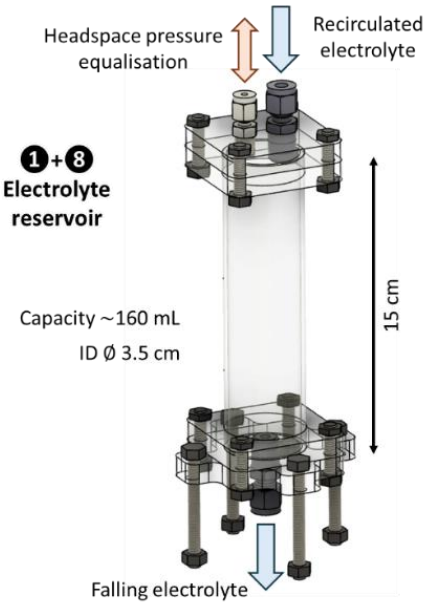

Fig. S 2 Illustrative diagram of the custom electrolyte reservoirs. Parts ❶ and ❽ in Fig. S 1 are shown. Electrolyte is fed into the top of the reservoir and removed from the bottom.

Experimental cell designs

Schematic diagrams of the custom cell designs are provided for reproduction. Numbers in text (such as ⑤ and ❺) cross-reference to the diagram in Fig. S 1 to contextualise connections.

Weir reservoirs

For flowing electrolytes under gravity whilst maintaining constant electrolyte elevation heads, custom reservoirs were designed and constructed from transparent acrylic. Schematic drawings are provided in Fig. S 3 with exact dimensions for reproduction. Acrylic tubing was purchased and cut to length, whereas planar parts were laser-cut or machined from sheet acrylic. All parts were assembled by use of Tensol 12 adhesive binder. Polypropylene compression fittings were employed for tubing connections and a silicone gasket with compression bolts were used for attaching the lids. The reservoirs feature a central 50 mm tube that is continuously overfilled to set a constant electrolyte head, and a 100 mm tube that is used for collection and electrolyte circulation. Each reservoir was initially filled with 300 mL of electrolyte resulting in a headspace volume of approximately 100 mL per reservoir. The headspace was designed to be low volume to minimise gaseous product dilution, because during electrolyser operation, the CO_2 exhaust was flowed through the combined reservoir headspace to enable detection of gas bubbles evolved at the cathode surface.

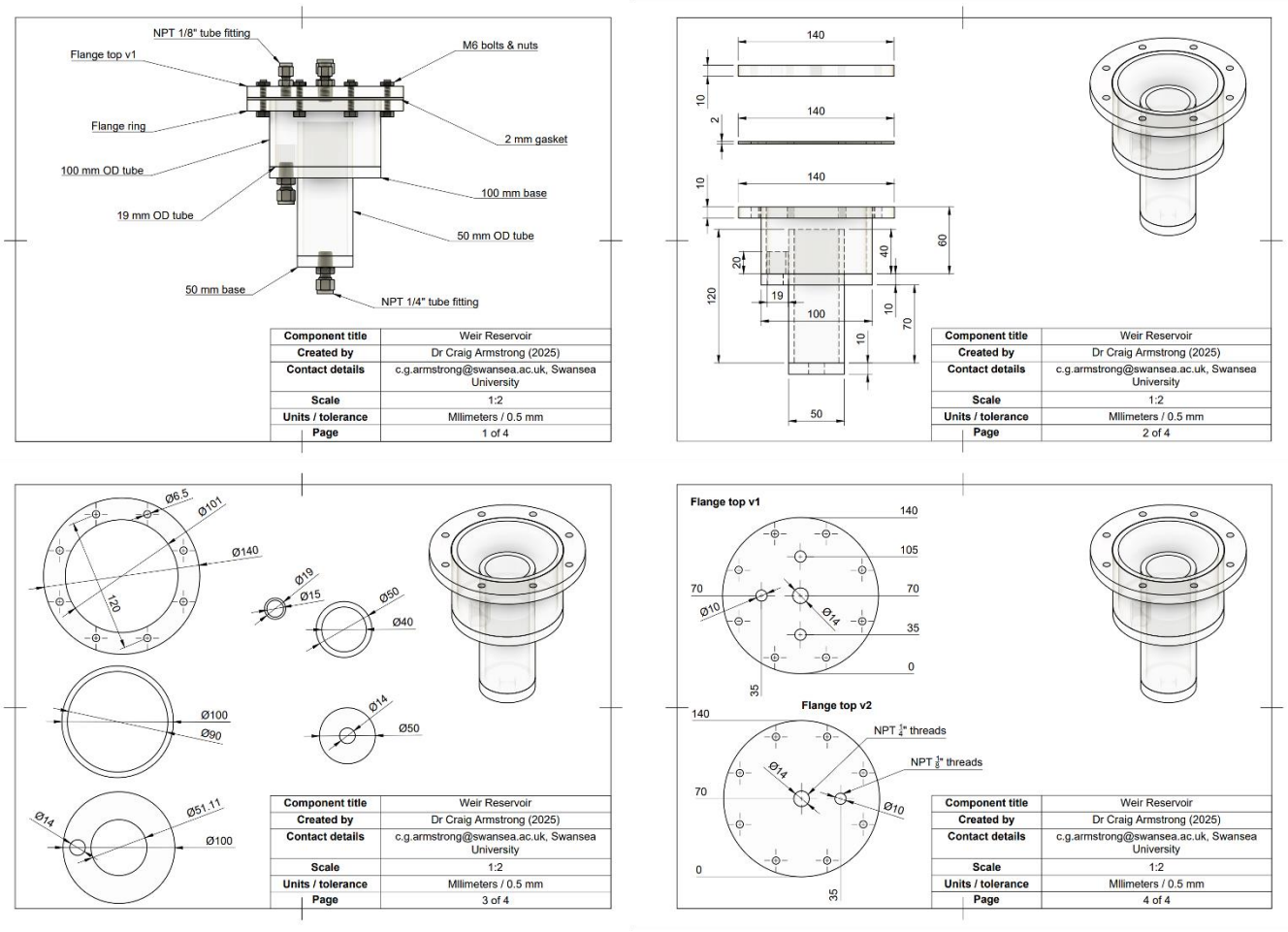

Fig. S 3 Schematic drawings of the 'weir' reservoirs employed for circulating electrolytes whilst maintaining constant electrolyte elevation heads. PDF versions are available on request from the authors.

40 x 5 cm² Hele-Shaw cell

For testing porous materials as percolators, a Hele-Shaw (H-S) cell was designed featuring pressure sampling points every 49 mm along its height. Schematic drawings are provided in Fig. S 4 with exact dimensions for reproduction. All parts were constructed by laser-cutting sheet acrylic, and compression bolts with silicone gaskets were used to seal the cell. Polypropylene compression fittings were employed for tubing connections and additional gaskets, and acrylic spacers were employed to vary the internal volumes and test different configurations such as the inclusion of a gas diffusion layer and flowing CO_2 gas. Pressure sampling points were connected to gauge (CO_2 ⑤ and electrolyte ❺) and differential pressure meters (⑧ and ❷) for measuring pressures within the cell chambers, and across the GDL interface. During operation, a 40 x 5 cm² sized percolator was housed entirely within the gaskets, whereas the gas diffusion layer was 45 x 6 cm² in size and positioned between gaskets. To prevent the GDL flexing upon pressurisation by liquid or gas, the reverse side of the GDL (the carbon substrate side) was reinforced using stiff copper mesh and additional acrylic inserts placed within the CO_2 chamber. 3D-printed flow-frame inserts were used to direct gas flow around the acrylic inserts and to diffuse gas to all areas of the GDL. The height of the H-S cell was limited to 40 cm by practical considerations as commercial GDLs that are readily available for purchase in academic research are typically limited to ~50 cm in length (a minimum length of 46 cm was required for gasketing in the H-S cell).

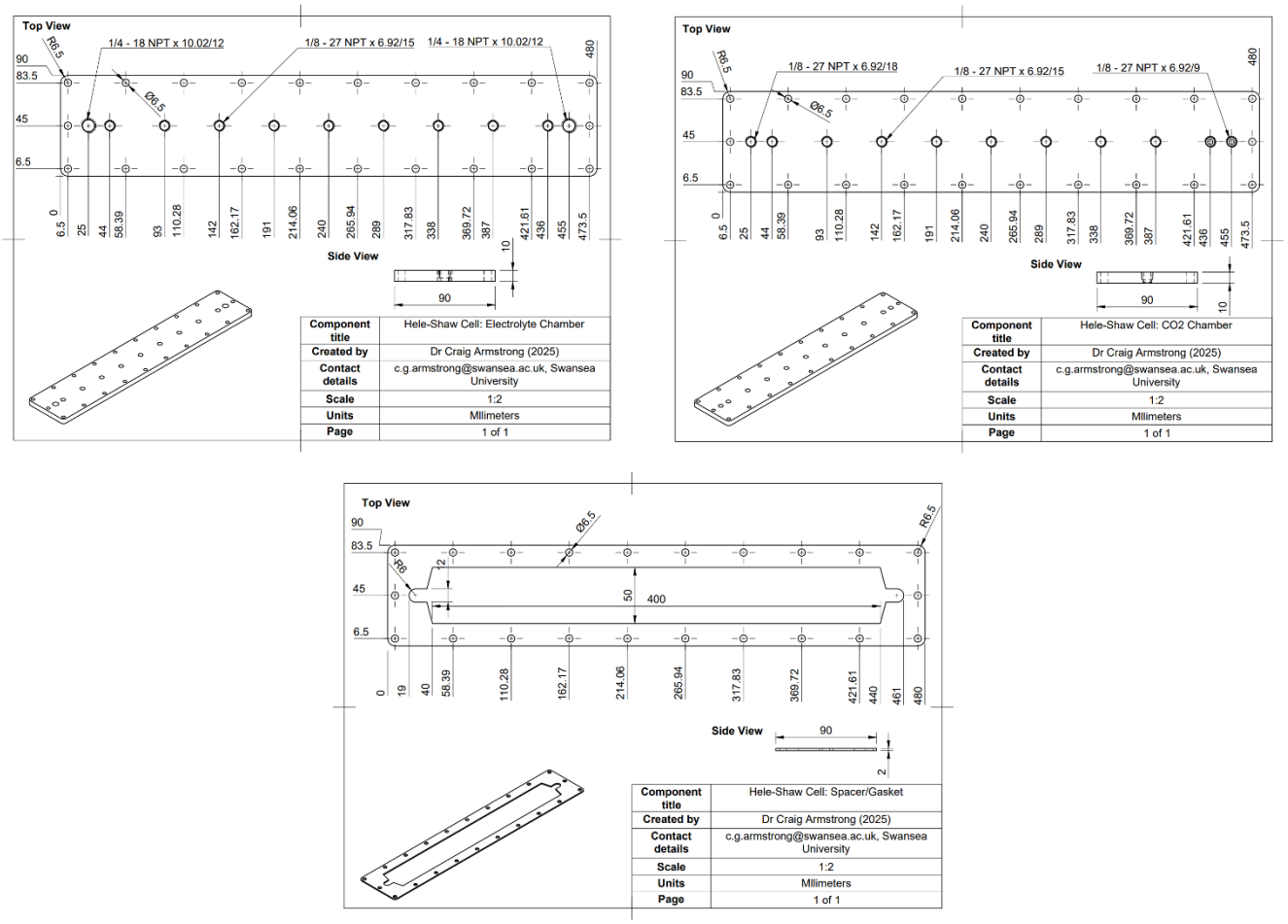

Fig. S 4 Schematic drawings of the H-S cell employed for differential pressure measurements. PDF versions are available on request from the authors.

3.16 x 3.16 cm² electrolysis cell

For differential pressure measurements, a conventional chambered electrolysis cell was designed and constructed from transparent acrylic with a square 10 cm² electroactive area. The design is illustrated in Fig. S 5 and exact dimensions are provided in Fig. S 6 for reproduction. The electrolysis cell is composed of three chambers for CO_2, catholyte and anolyte, each with a unique internal shape that was designed to remove gas bubbles and flooded electrolyte by buoyancy and gravity, respectively. Correspondingly, the flow directions of gas and electrolytes to achieve efficient removal are shown in Fig. S 9b and Fig. S 10b respectively. The electrolysis cell features a square 3.16 x 3.16 cm² electroactive area and is designed to fit electrodes and membranes of size 5 x 5 cm², allowing space for gasket sealing. For connection to a potentiostat, adhesive copper tape was used as current collector material that was affixed to 2 mm thick acrylic spacers. Electrical contact between the current collector and reverse side of electrodes was achieved by cell compression. Due to the shape of the drainage chambers, additional acrylic spacers of 1 mm thickness and silicone gaskets were required to ensure full gasket compression of the top and bottom of electrodes. Differential pressure at the GDE interfaces were probed by connection of the differential pressure meter (⑧ and ❷) to the ports annotated in Fig. S 5b.

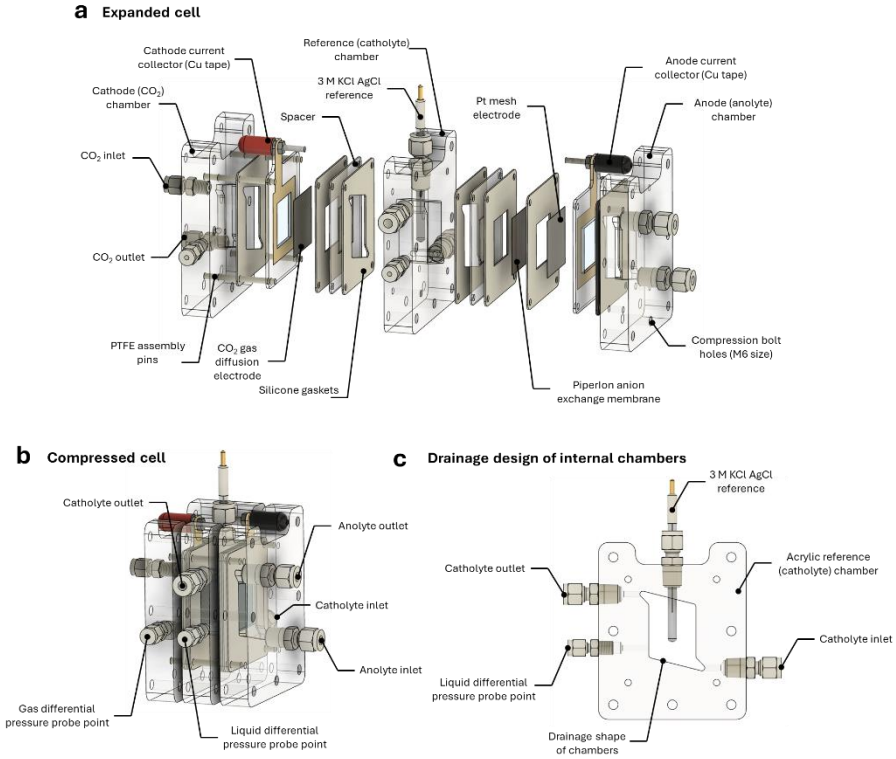

Fig. S 5 Illustrative diagram of the 3.16 x 3.16 cm² chambered electrolysis cell, showing all components annotated. M6 compression bolts and nuts are omitted for clarity. (a) Expanded view, (b) compressed view and (c) drainage design.

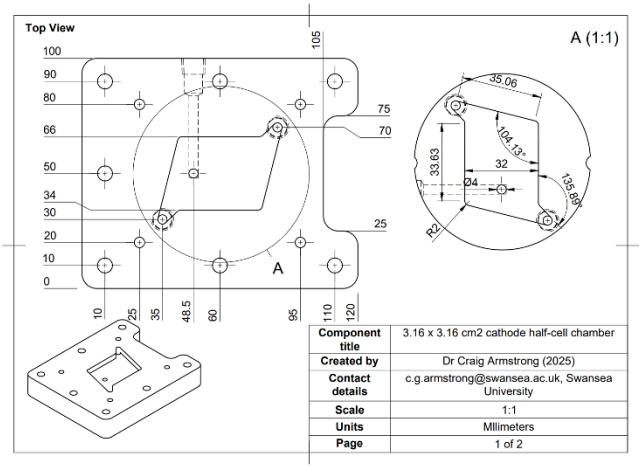

Component title	3.16 x 3.16 cm2 cathode half-cell chamber
Created by	Dr Craig Armstrong (2025)
Contact details	c.g.armstrong@swansea.ac.uk, Swansea University
Scale	1:1
Units	Millimeters
Page	1 of 2

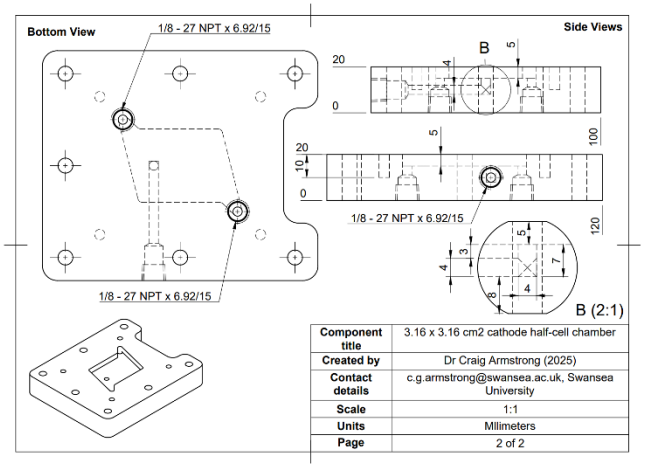

Component title	3.16 x 3.16 cm2 cathode half-cell chamber
Created by	Dr Craig Armstrong (2025)
Contact details	c.g.armstrong@swansea.ac.uk, Swansea University
Scale	1:1
Units	Millimeters
Page	2 of 2

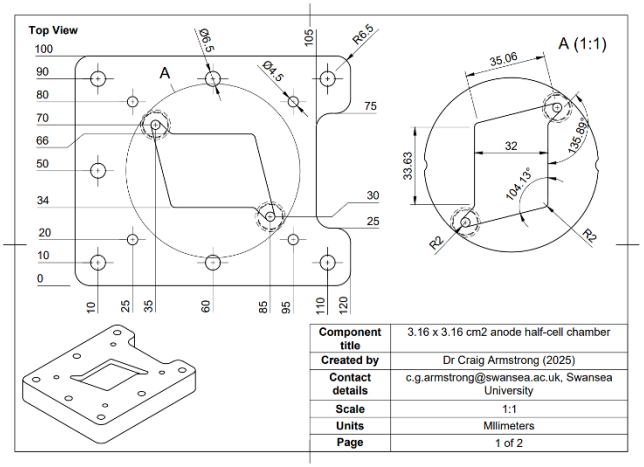

Component title	3.16 x 3.16 cm2 anode half-cell chamber
Created by	Dr Craig Armstrong (2025)
Contact details	c.g.armstrong@swansea.ac.uk, Swansea University
Scale	1:1
Units	Millimeters
Page	1 of 2

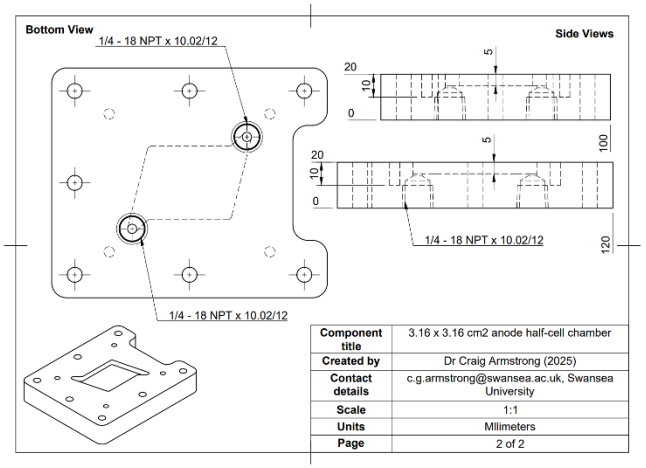

Component title	3.16 x 3.16 cm2 anode half-cell chamber
Created by	Dr Craig Armstrong (2025)
Contact details	c.g.armstrong@swansea.ac.uk, Swansea University
Scale	1:1
Units	Millimeters
Page	2 of 2

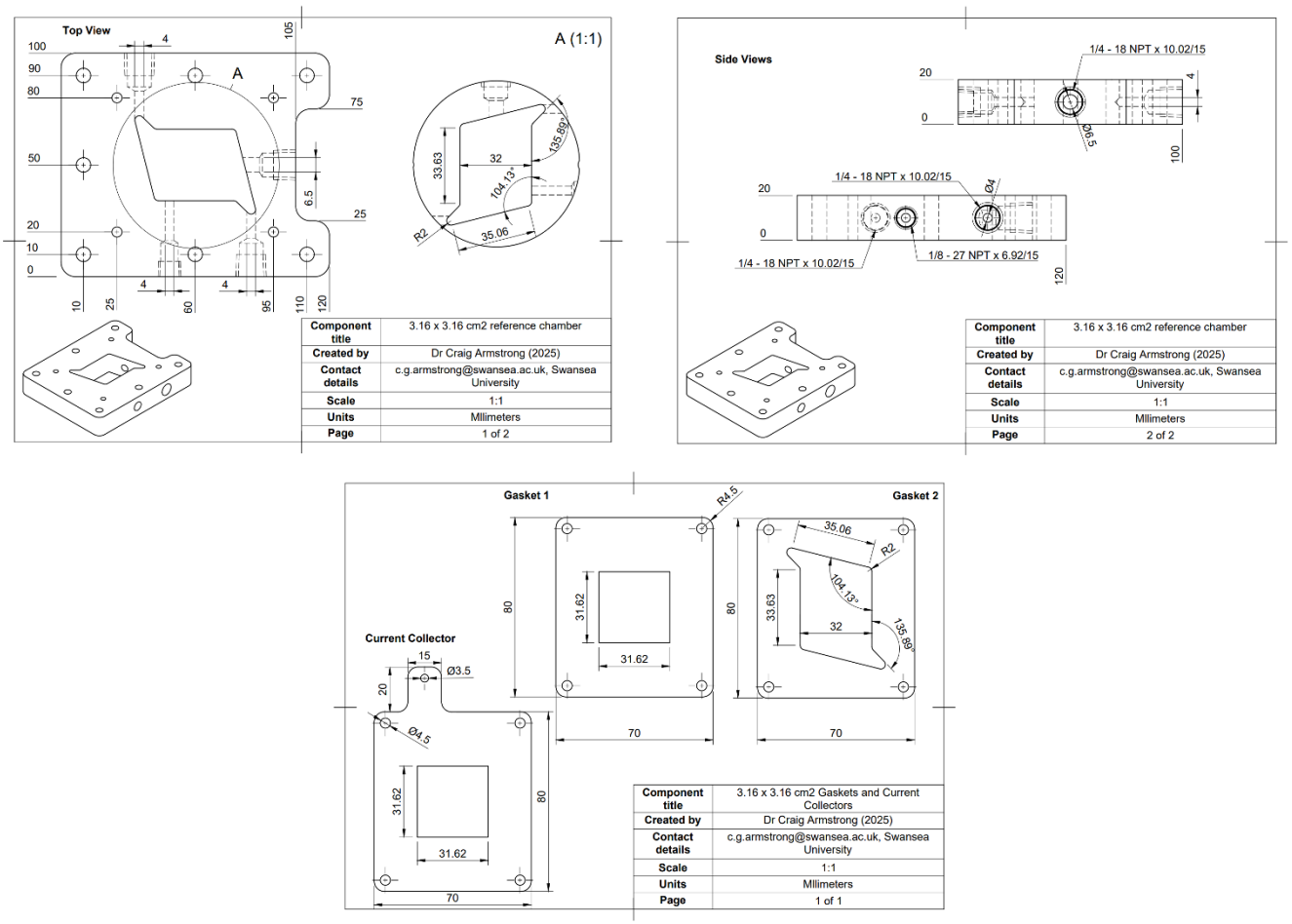

Fig. S 6 Schematic drawings of the 3.16 x 3.16 cm^2 chambered electrolysis cell. Dimensions are provided for the cathode, reference and anode chambers, which flow CO_2, catholyte and anolyte respectively. PDF versions are available on request from the authors.

32 x 1 cm^2 falling-film electrolyser

To demonstrate the operation of a falling-film electrolyser (FFE) for CO_2 reduction, a tall electrolysis cell was developed featuring a flow frame for housing a percolator material and pressure sampling points for measuring pressure balance as a function of height. Schematics for the design are provided in Fig. S 7 for reproduction. The electrolysis cell was composed of three chambers for CO_2, catholyte and anolyte, and operated an electrode area of 32 x 1 cm^2. The cell frames were machined from transparent acrylic and possessed recesses for nitrile rubber O-rings placed between the cell frames and current collectors. For connection to a potentiostat, adhesive copper tape was applied to the acrylic current collectors. Electrical contact between the current collector and reverse side of electrodes was achieved by cell compression. Each current collector also featured a 1 mm deep slot for flow which enabled CO_2 to flow behind the GDE cathode, and anolyte to flow behind and through the nickel foam anode. Placed between the cathodic and anodic current collectors, a 3D-printed flow frame was positioned that featured a central void filled with percolator material, and side channels that enabled pressure measurement of the catholyte chamber. These probing channels continued through the cathodic current collector and cell frame, where connections to the differential pressure meter were made (⑧ and ❷). To reinforce the ion-conductive membrane, the nickel foam anode was assembled directly against the membrane in a zero-gap configuration.

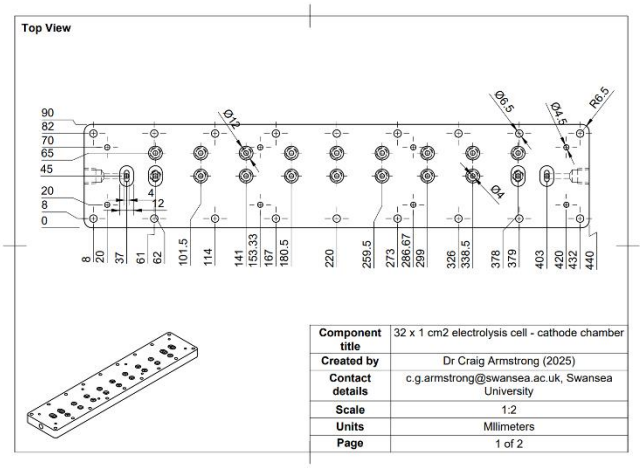

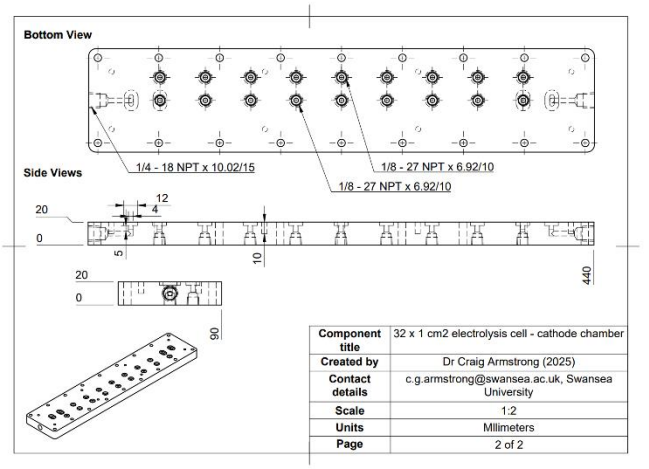

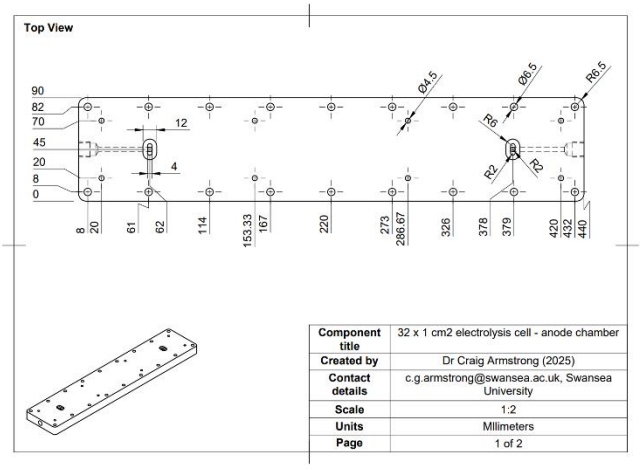

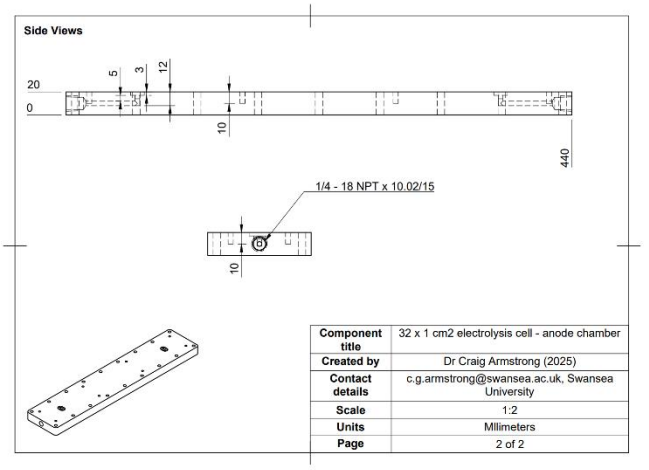

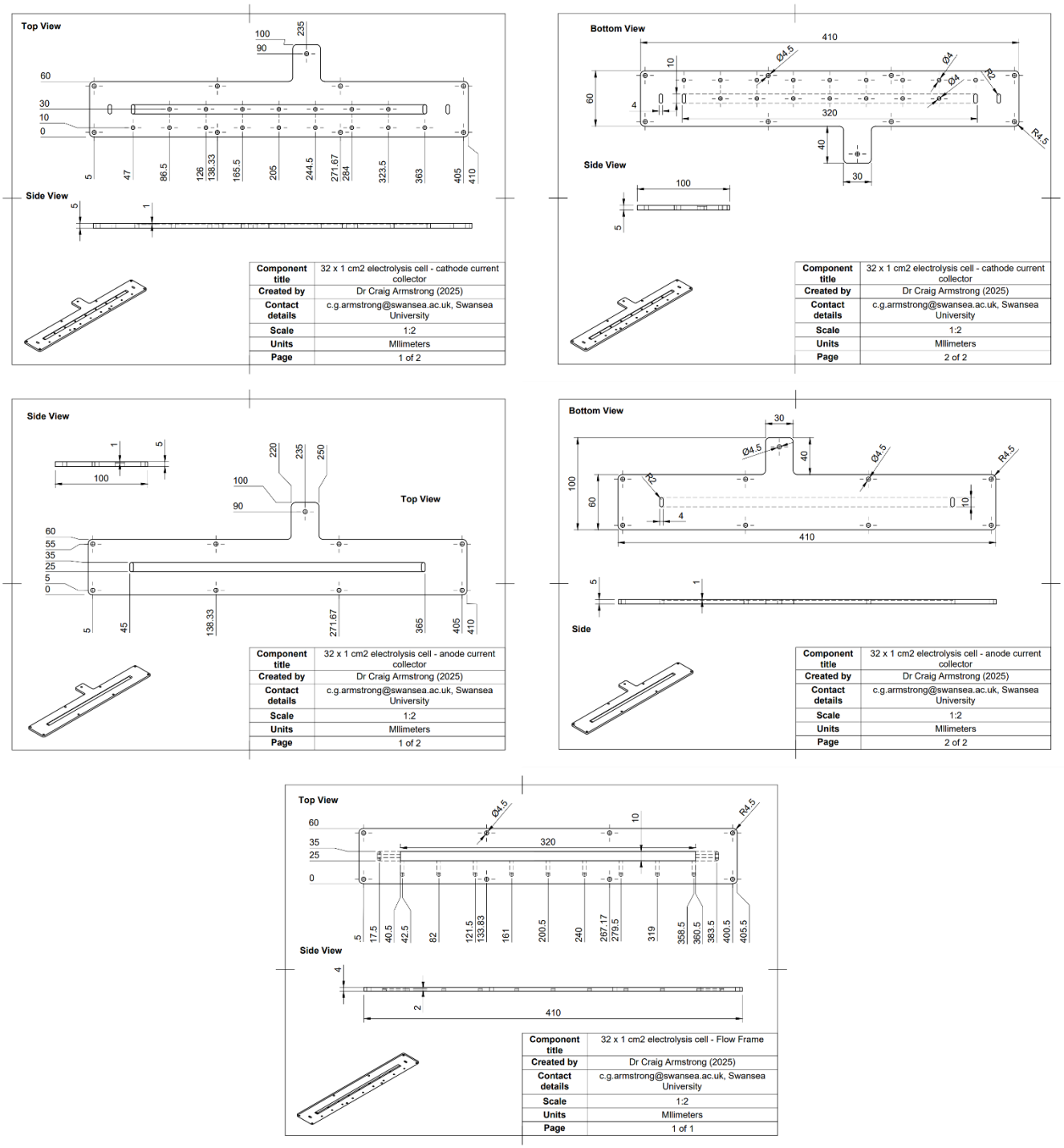

Fig. S 7 Schematic drawings of the 32 x 1 cm^2 percolated falling film electrolysis cell. Dimensions are provided for the cathode and anode chamber, the current collectors and flow-frame, which flow CO_2, anolyte and percolated catholyte respectively. PDF versions are available on request from the authors.

Electrolyte and gas circulation

40 x 5 cm² Hele-Shaw cell

For the measurement of vertical pressure distribution, the H-S cell was employed using CO_2 and electrolyte circulation as shown in Fig. S 8. Electrolyte was circulated through the cell using the weir reservoirs described above and a circulation pump was used to keep electrolyte heads constant during differential pressure measurements. The electrolyte chamber was filled with either the polypropylene or polyurethane percolator materials. When employing a GDL for two compartment measurements, a CO_2 chamber was added with CO_2 flowing behind the GDL at 100 mL min^{-1}. Percolators had to be pre-soaked before assembly into the H-S cell to ensure reliable and saturated electrolyte flow due to the polymeric materials being resistant to wetting and prone to withholding air bubbles. The use of a pump to fill the cell upwards, as in the porous flow experiments, was attempted but ultimately ill-advised because of the excessive pressure generated by the flow resistive percolator. This resulted in immediate GDL flooding and tearing of the thin GDL material. The use of an elastic element was required to prevent GDL deformation and voids forming between the percolator and GDL, as this created pathways for faster flow and a negative pressure gradient akin to the case of gravity flow without a percolator.

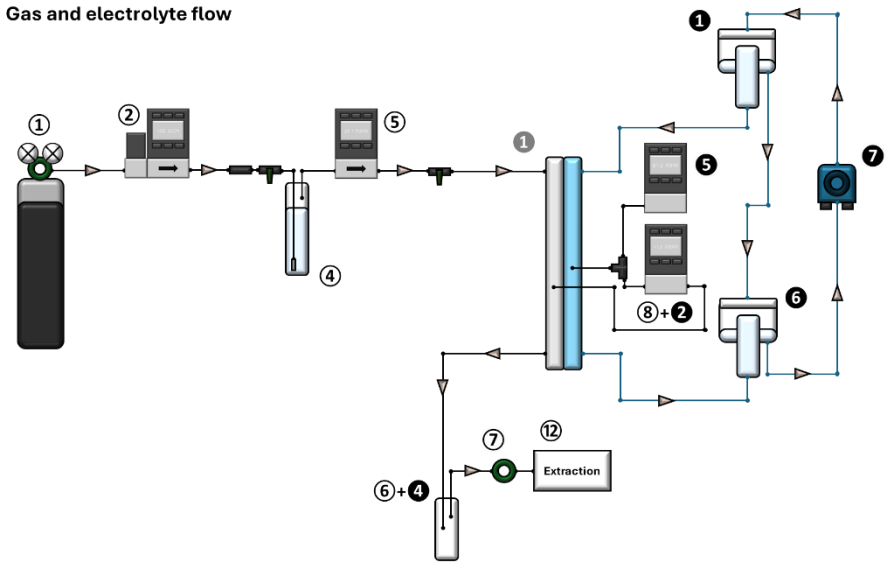

Fig. S 8 Schematic illustration of the electrolyser platform showing the paths of CO_2 and electrolyte for differential pressure measurements within the Hele-Shaw cell with a gravity-driven flow. Numbers refer to the key in Fig. S 1 (also see manuscript diagram) and arrows indicate the flow directions. Black lines represent CO_2 flow, and blue lines show catholyte flow.

3.16 x 3.16 cm^2 electrolysis cell

CO_2 flow through the electrolyser platform is summarised in Fig. S 9. The CO_2 was sourced from a cylinder ① (zero grade, British Oxygen Company Ltd.) and fed into two mass flow controllers ② and ③, used as independent reactant and purge gasses set at flow rates of 100 and 200 - 400 mL min^{-1}, respectively. The reactant gas was bubbled through a humidification column ④ and then through a gas pressure meter ⑤ and finally delivered to the electrochemical cell CO_2 inlet 1. The product gas then flowed from the cell outlet through the catch reservoir ⑥/4 and then the backpressure regulator ⑦ (Swagelok), which was used to control the CO_2 pressure within the gas chamber of the electrochemical cell. Meanwhile, the purge gas was flowed through a separate humidification column ④ and unified with the product gas stream in the lower catholyte reservoir headspace 6. From here, the combined product and purge gas flowed through a moisture trap ⑨ (Drierite, Fisher Scientific) to remove humidity, then a mass flow meter ⑩ and finally to the gas chromatograph (GC) ⑪ via an exhaust bypass. The purge gas was used for two purposes: firstly, to saturate the system with CO_2, and secondly to generate enough flow pressure at the GC inlet to push sample through the instrument inlet. It was found that if the entire gas stream was forced through the GC, then the GC inlet/outlet valves would generate excessive back pressure on the electrolyser platform and severely restrict flow rates. Thus, an exhaust bypass was required to divert most gas flow to extraction ⑫. In Fig. S 9, all gaseous tubing had an internal diameter of 1.6 mm to minimise internal volume.

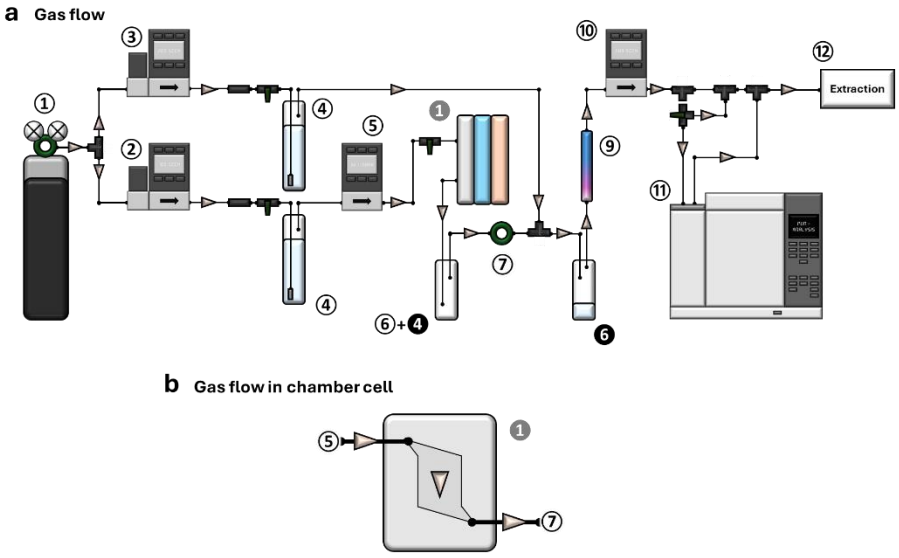

Fig. S 9 (a) Schematic illustration of the electrolyser platform showing the path of gas flow from cylinder source to gas chromatograph and extraction. Numbers refer to the key in Fig. S 1 and arrows indicate the flow direction; (b) The flow direction of the reactant CO_2 gas through the 3.16 x 3.16 cm^2 chamber flow cell. The downwards flow is intended to clear any flooding electrolyte from the flow cell.

Electrolyte flow through the electrolyser platform is summarised in Fig. S 10. The catholyte and anolyte fall from the upper reservoirs 1 and 8 down to the lower reservoirs 7 and 10 via the electrochemical cell 1. The electrolytes are then recirculated back to the top reservoirs independently by two microfluidic gear pumps (MGD1000P-PK-V-EQI, TCS Micropumps Ltd.), each operating at approximately 6000 rpm. The pumps were operated at a flow rate far exceeding the gravity-fed flow rate such that all electrolyte was housed in the upper reservoirs 1 and 8 and the liquid levels remained constant during experiments. The flow rates of the falling catholyte and anolyte were independently adjusted by use of flow restrictors/meters 3 and 9. During electrolysis, the flow rates were set to 100 mL min^{-1}, however deviation occurs during operation due to the uncontrolled nature of the gravity-driven flow and pressure effects of the GDE. To measure the electrolyte pressure exerted on the GDE, a liquid pressure meter 5 was mounted at the same height as the GDE and was fed with flowing catholyte on a bypass loop. In contrast, a differential pressure meter ⑧/2 was directly connected to the electrolysis cell 1 catholyte and CO_2 chambers to probe the differential pressure at the GDE interfaces. The tubing between the electrolysis cell and the differential pressure meter were non-flowing and air-filled. Connections to the chamber flow cell were made in a reverse upwards flowing direction, as depicted in Fig. S 10b, to facilitate the removal of gas bubbles. Electrolyte tubing had an internal diameter of 3.2 mm, excluding the pressure meters 5, ⑧ and 2 which had a 1.6 mm internal diameter.

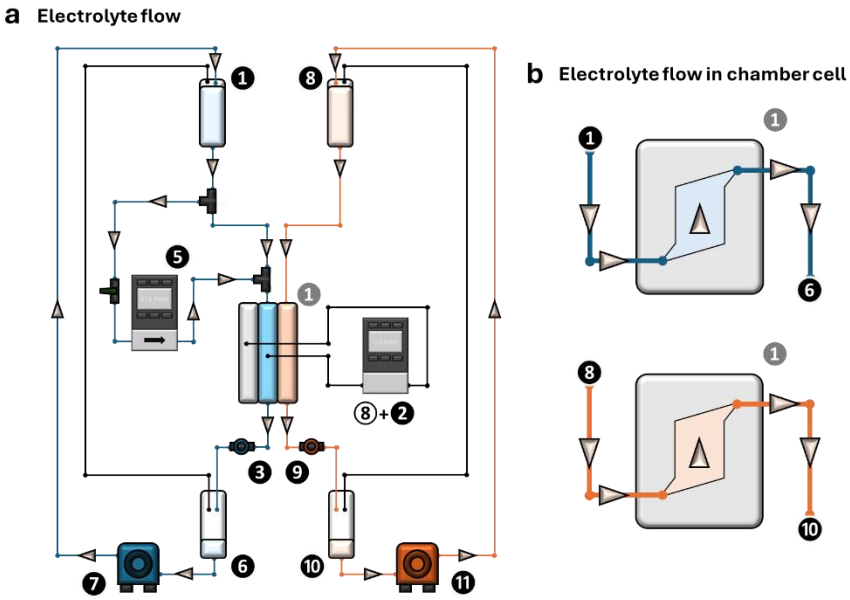

Fig. S 10 (a) Schematic illustration of the electrolyser platform showing the paths of catholyte and anolyte flow. Numbers refer to the key in Fig. S 1 and arrows indicate the flow directions. Black lines represent gas tubing connections between the lower and upper reservoir headspaces, and the electrochemical cell CO_2 and catholyte chambers to the differential pressure meter. The catholyte circuit is indicated in blue whereas the anolyte circuit is indicated in orange; (b) The flow directions of the catholyte and anolyte through the 3.16 x 3.16 cm^2 chamber flow cell. This upwards reverse flow is intended to clear gas bubbles from the flow cell.

Threshold pressures for GDE gas breakthrough and electrolyte flooding were measured on a small scale using the electrolysis cell shown in Fig. S 5, and GDLs/catalyst GDEs of size 10 cm^2 exposed area. The cell was modified by removal of unnecessary components (reference electrode, membrane, counter electrode and current collectors) and by plugging the unused fittings (reference electrode port, anolyte inlet and outlet). This effectively changed the cell into a two-chamber design (CO_2 and catholyte) separated by the GDE and provided transparent windows for observation of gas bubble and electrolyte droplet formation. The flow of electrolyte through the apparatus was also modified to give direct control of the liquid pressure as shown in Fig. S 11. Here electrolyte was pumped upwards through the catholyte chamber, and a pin valve (Swagelok) was used to introduce back-pressure on the catholyte chamber against the pump. In addition, a single reservoir of electrolyte was employed and positioned above the cell (liquid level approx. 50 cm above) to give a constant positive hydrostatic pressure on the cell. During operation, CO_2 and electrolyte were fed and pumped respectively into the cell at a constant flow rate of 100 mL min^{-1}. The threshold gas breakthrough differential pressure was measured by fixing the electrolyte pressure and slowly increasing the CO_2 back-pressure until the first visible bubble of emergent CO_2 was observed. Likewise, the threshold electrolyte flooding pressure was measured by fixing the CO_2 pressure and increasing the electrolyte back-pressure until the first visible droplet of emergent electrolyte was observed.

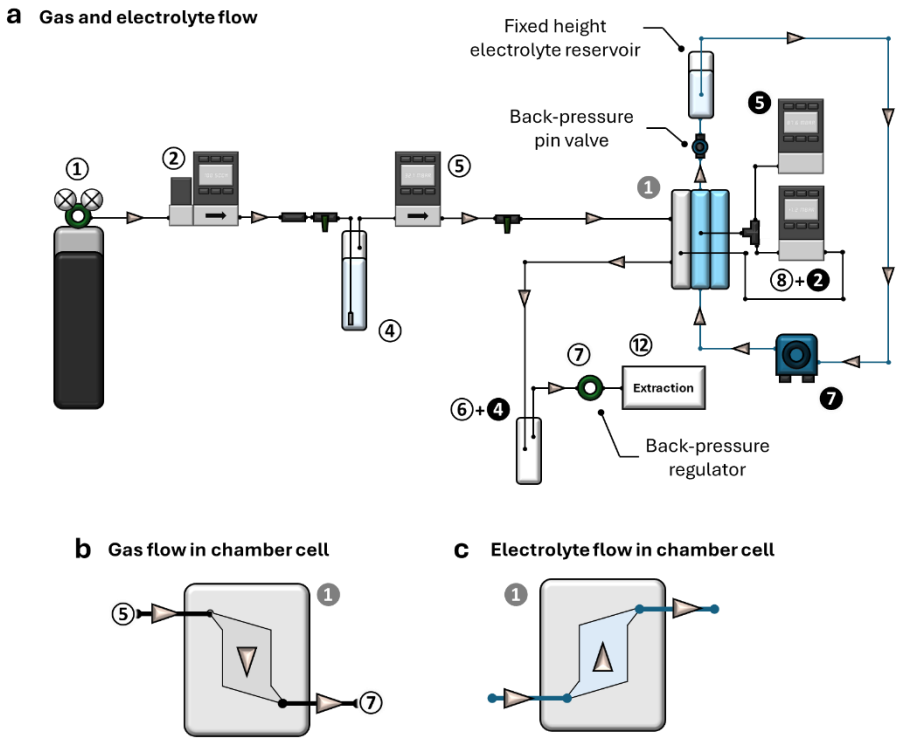

Fig. S 11 (a) Schematic illustration of the electrolyser platform showing the paths of CO_2 and electrolyte for threshold differential pressure measurements. Numbers refer to the key in Fig. S 1 and arrows indicate the flow directions. Black lines represent CO_2 flow, and blue lines show electrolyte flow. The flow directions of the CO_2 and electrolyte through the 3.16 x 3.16 cm^2 chamber flow cell are shown in (b) and (c).

32 x 1 cm² falling-film electrolyser

For EC-CO_2R electrolysis using the percolated FFE 32 x 1 cm² flow cell, the platform was configured as shown in the photograph in manuscript and diagrammatically in Fig. S 12. CO_2 flow proceeded as in the other experiments above. Catholyte was circulated through the cell using the weir reservoirs described above via gravity. In contrast, the anolyte was circulated using a gear pump and pumped upwards through the anode chamber at 100 mL min^{-1} from a larger reservoir with 600 mL electrolyte volume. For probing the GDE vertical pressure balance, two differential pressure meters (⑧ + ❷) were used and attached to the top and bottom of the electrolyser.

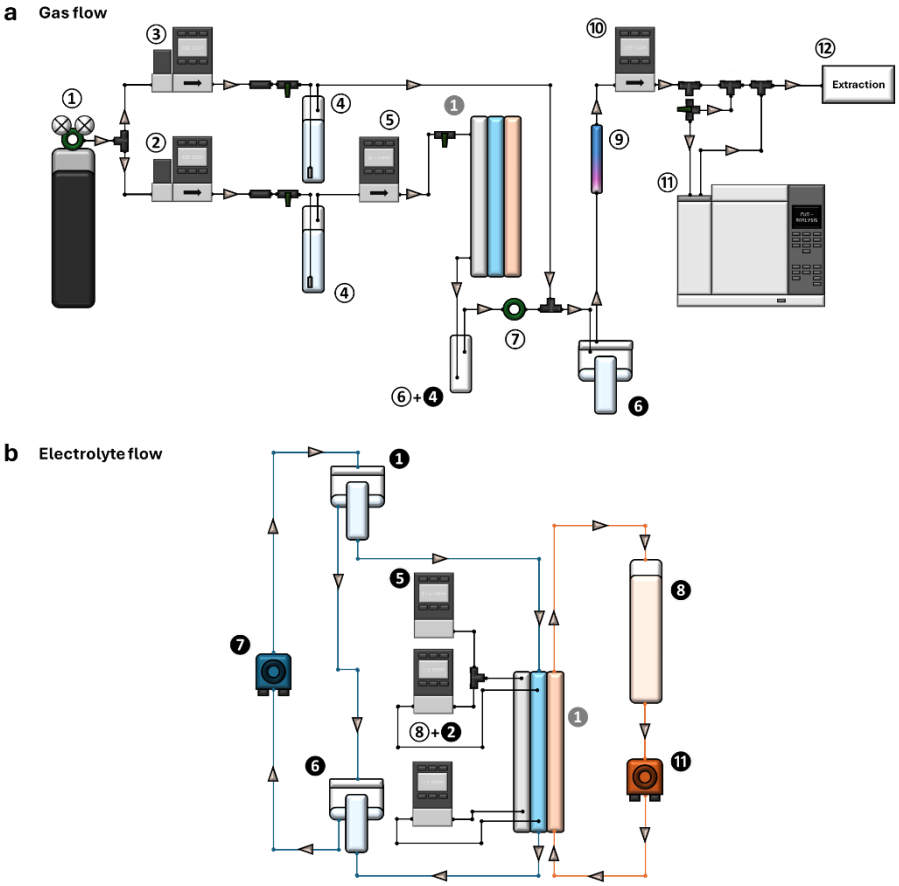

Fig. S 12 Schematic illustration of the electrolyser platform showing the paths of (a) CO_2 and (b) electrolyte for EC-CO_2R electrolysis using the 32 x 1 cm² flow cell. Black lines represent CO_2 flow, and gravity-driven catholyte flow is shown in blue whereas pumped anolyte flow is shown in orange. Numbers refer to the key in Fig. S 1 (also see manuscript diagram), and arrows indicate the flow directions.

Pressure measurements

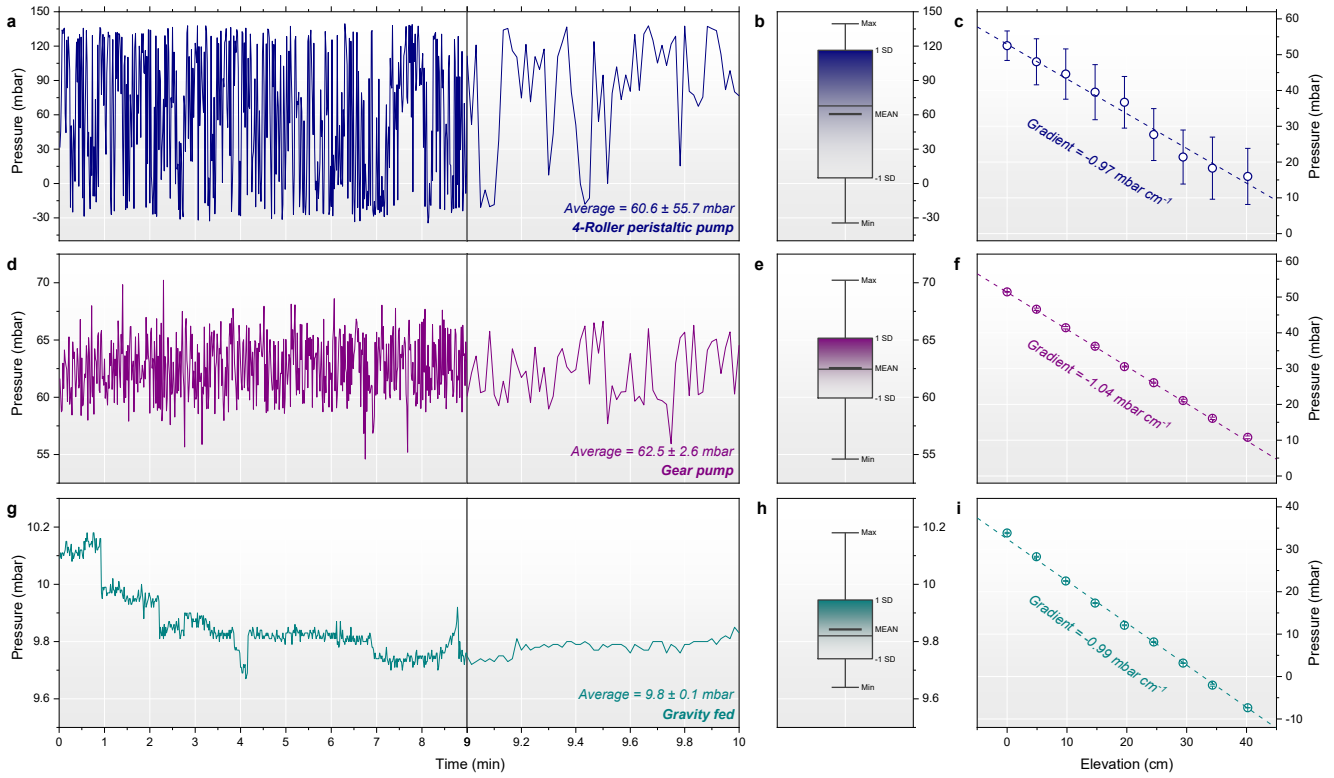

Fig. S 13 Pressure fluctuations associated with different electrolyte circulation methods over a 10-minute period, with fluctuations highlighted between 9 and 10 min. (a) A 4-roller peristaltic pump is compared to (d) a hydraulic gear pump and to (g) a gravity-fed electrolyte. A statistical analysis of each recirculation method is represented by box charts in (b), (e) and (h). In (c), (f) and (i), the vertical pressure distribution is plotted with error bars corresponding to the standard deviations of fluctuations. In each case the internal tubing diameter was 3.175 mm and the electrolyte was pumped or fed at 100 mL min^{-1} from a feed reservoir arbitrarily at 1.5 m elevation (approx. 0.5 m higher than the base of the H-S cell). In (a) and (d) the electrolyte was pumped upwards whereas in (g), the electrolyte was flowed downwards to a lower drain reservoir at 1 m elevation, and the flow rate was restricted using an analogue flow meter. Pressure measurements were recorded in-line (electrolyte flowed directly through the pressure sensor) in (a), (d) and (g), whereas they were probed within the H-S cell (via a connecting air-filled tube) in (c), (f) and (i), causing notable pulsation dampening in the (c), (f) and (i) data.

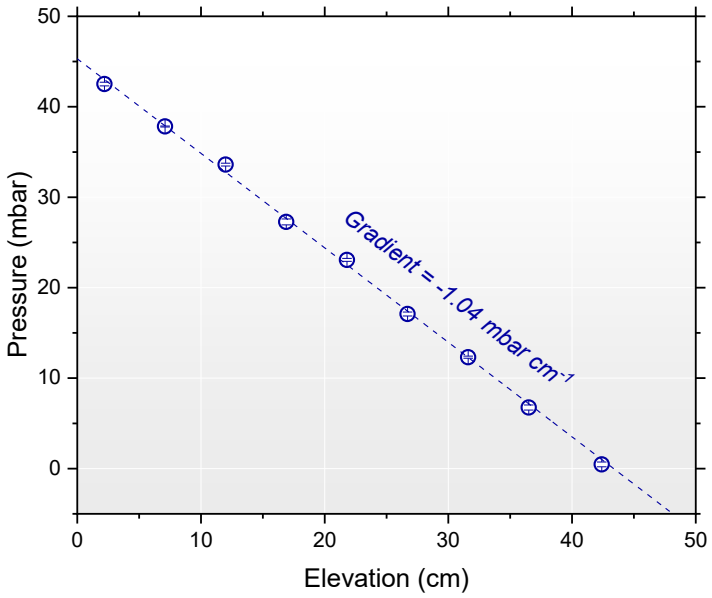

Fig. S 14 Graph showing the control experiment whereby the vertical pressure distribution under static conditions and without a percolator material is measured. Data points show the average pressure over three repeats with associated error bars indicating the experimental standard deviation.

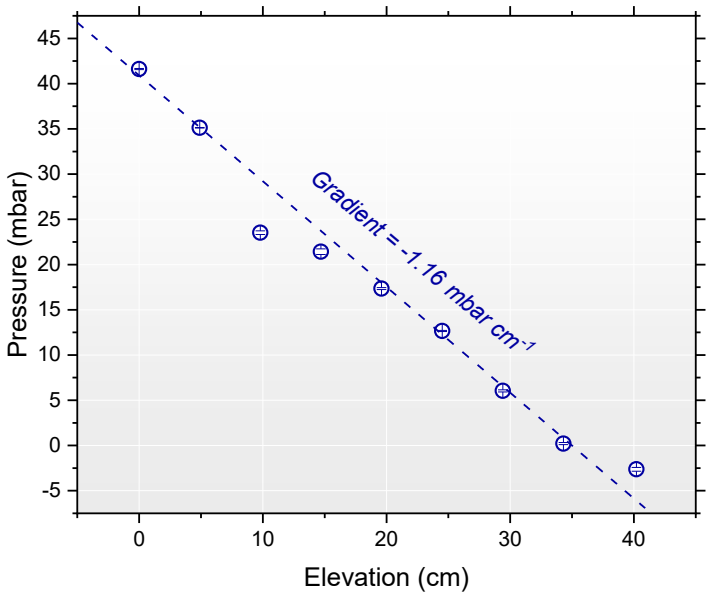

Fig. S 15 Graph showing the control experiment whereby the vertical pressure distribution under unrestricted gravity falling electrolyte without a percolator material is measured. Data points show the average pressure recorded over 2 minutes with associated error bars indicating the standard deviation.

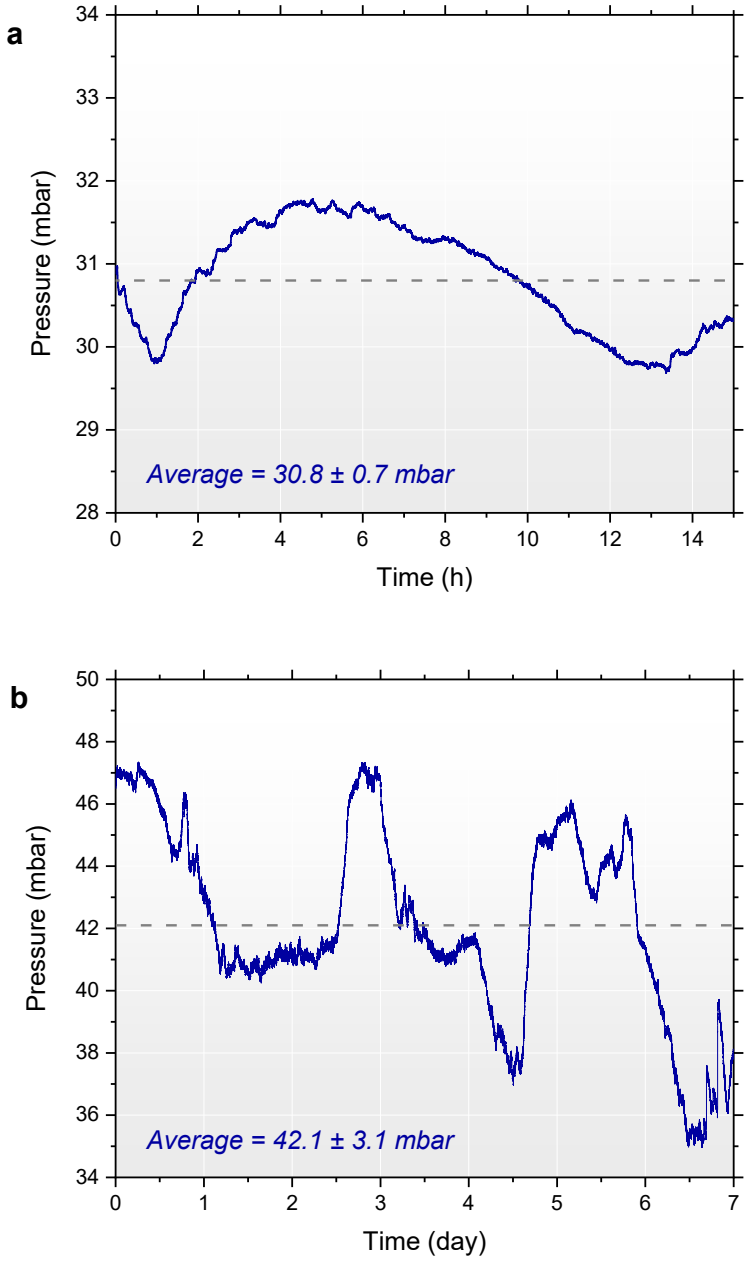

Fig. S 16 Pressure monitoring of the H-S cell featuring a polypropylene percolator, circulated using the weir reservoirs, over (a) 15 hours and (b) 7 days. The horizontal dashed line shows the average pressure.

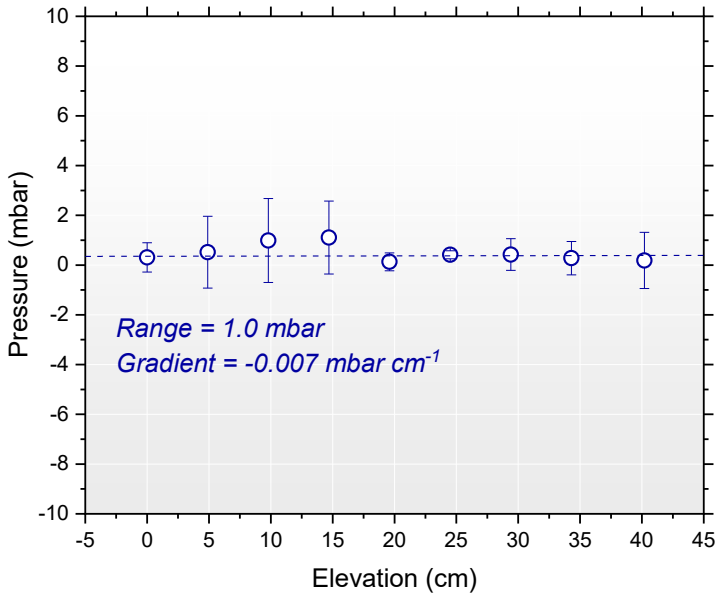

Fig. S 17 Vertical pressure distribution along a 40 cm polyurethane foam percolator; 1 layer compressed within a 4 mm gasket. The reservoirs were configured with $\Delta z_{\mathrm{Res}} = L$ and then head losses were empirically compensated to give a constant pressure distribution at zero-gauge pressure. Datapoints give the average pressure of three repetitions and experimental standard deviations are shown as error bars.

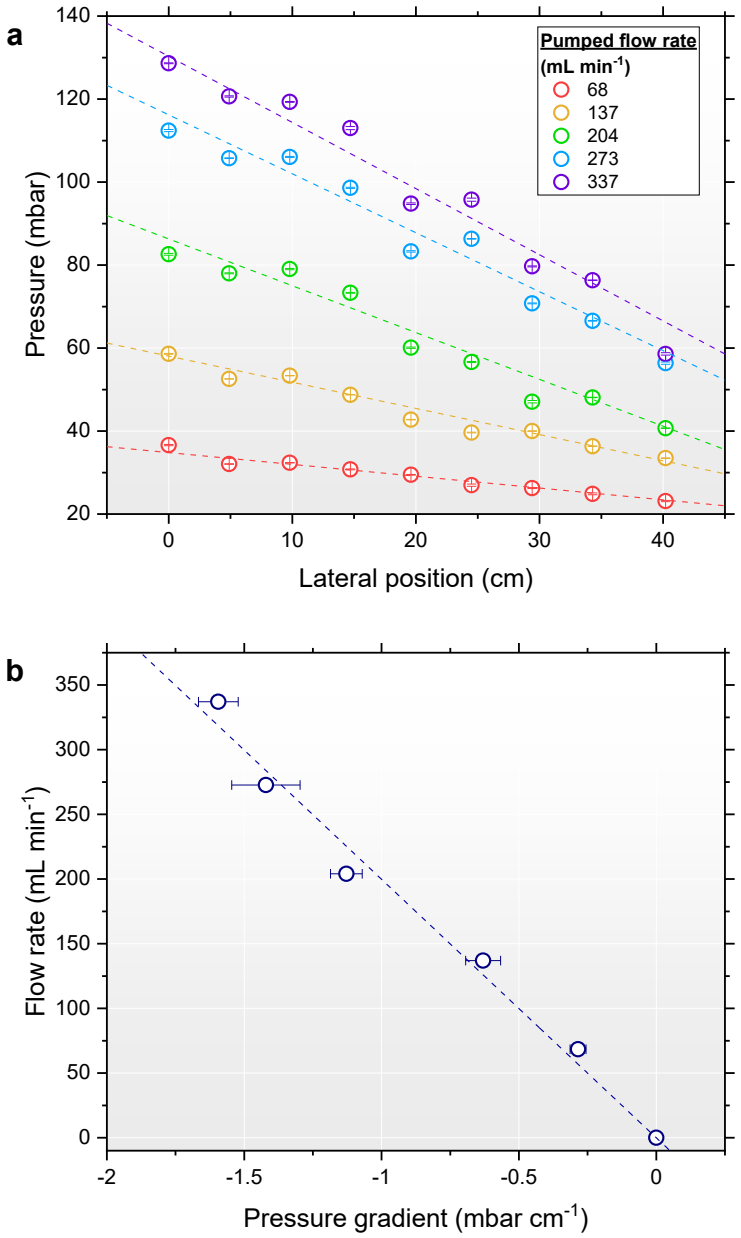

Fig. S 18 Determination of the effective permeability of the polyurethane foam percolator (1 layer compressed within a 4 mm gasket); (a) The pressure drop recorded at different flow rates. Error bars represent the standard deviation of the pressure recorded for 2 minutes; (b) A plot of the pressure gradients in (a) vs the applied flow rate. Error bars represent the standard errors of the gradients in (a), and linear regression is performed with the intercept set at the origin.

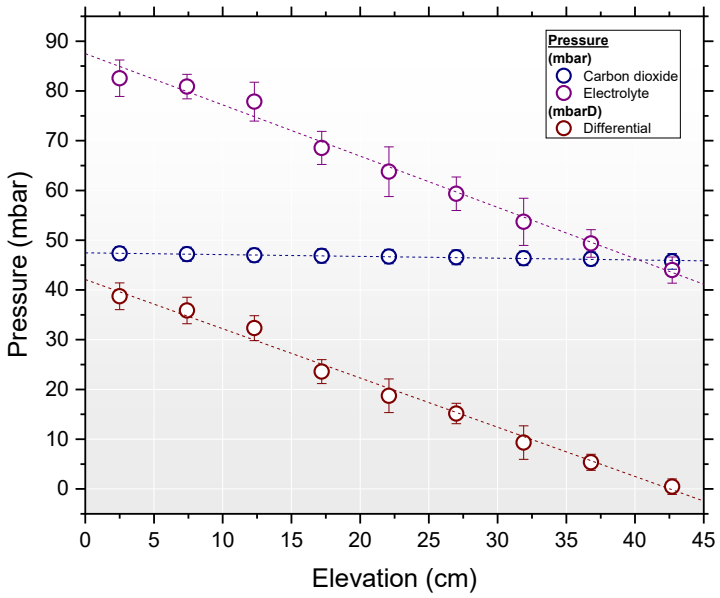

Fig. S 19 The pressure distribution recorded across a 45 cm height Sigracet 28BC GDL as a function of elevation. The gas pressure was adjusted to be equal to the electrolyte pressure at the top of the GDL, giving a balanced $\Delta P = 0$ mbar at that point. Datapoints give the average pressure of three repetitions and experimental standard deviations are shown as error bars.

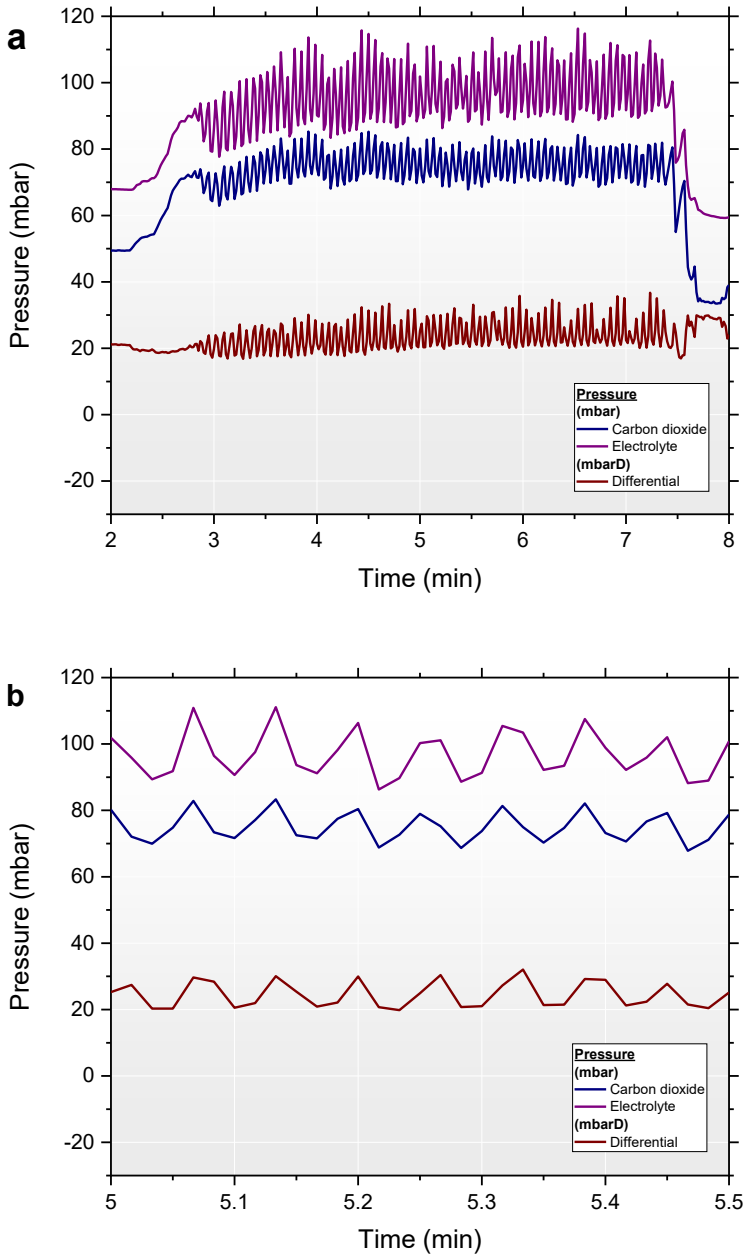

Fig. S 20 Pressure fluctuations observed at the mid-height of a 45 cm height GDL upon pumping electrolyte upwards without a percolator. A magnified view of the data at 5 min in (a) is shown in (b).

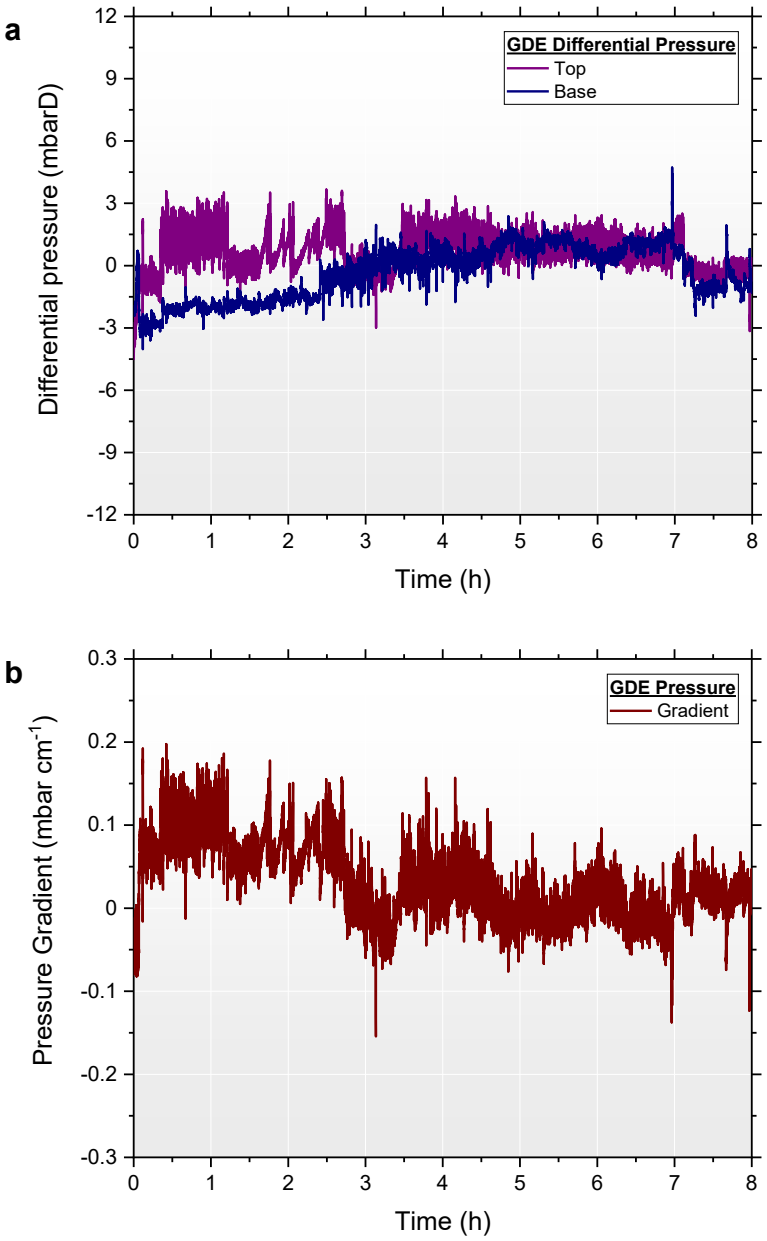

Fig. S 21 Control experiment using the 32 x 1 cm^2 FFE cell, featuring a polyurethane foam percolator, whereby the pressure across the height of the GDE was monitoring for 8 h. Catholyte was circulated under gravity using the weir reservoirs with head losses compensated. CO_2 was flowed continuously through the gas chamber, and the CO_2 pressure was preconfigured to be equal to the electrolyte pressure giving $\Delta P \cong 0$ mbarD. (a) Differential pressures as the top and base, and the (b) vertical pressure gradient are shown as a function of time.

Gas diffusion electrode characterisation

preparation

GDEs featuring a silver nanoparticle catalyst layer were prepared by airbrush spray-coating a catalyst ink composed of commercial silver nanoparticles (20 – 40 nm, 99.9 %, Thermo Scientific) and Nafion® D-520 dispersion (5% w/w in water and 1-propanol, Tygrave Enterprises Ltd.) used as a binder and ion-transport medium. A catalyst loading of 1 mg cm^{-2} was targeted for all GDE employed in this study. The method for ink preparation and spray-coating (for a 34 x 3 cm^2 GDL) was as follows:

20 g of water (ultrapure deionised) was added to 20 g of isopropanol (HPLC grade) and stirred in a 100 mL DURAN® glass bottle. To which, 2 g of Nafion® D-520 dispersion was then added and stirred until fully dissolved. 600 mg of silver nanoparticle powder was then added to the solvent-Nafion mixture and then sonicated for 20 minutes using a Cole-Parmer® 500-Watt Ultrasonic Processor and ¼" probe, whilst stirring. To avoid the over-heating of the probe and ink, the mixture was sonicated at 30 % amplitude with an intermittent program (10 s on time then 10 s off time, for a total time of 40 minutes), resulting in a maximum ink temperature of approximately 60 °C. After cooling, the entire ink mixture was then immediately spray-coated onto a pre-weighed GDL, which was suspended onto a large hotplate (Fisher Scientific) set at 140 °C within a fume-cupboard, using a wide-angle airbrush (Gaahleri premium series GHPM-Mobius TG 0.5 mm airbrush using 2 bar compressed air) (Fig. S 22a). The airbrush featured a 20 mL gravity cup, thus requiring approximately 4 aliquots of ink to dispense the entire mixture. The spray-coating process was completed in approximately 30 minutes, during which time the ink mixture was continuously stirred between gravity-cup aliquots. The airbrush was manually operated by passing back-and-forth over the GDL sample (approximately 15 cm above) in a repetitive pattern, whilst pausing as needed to allow solvent evaporation. The GDE was then fully dried on the hotplate for 10 minutes under fume-cupboard air flow before weighing to calculate the associated catalyst loading.

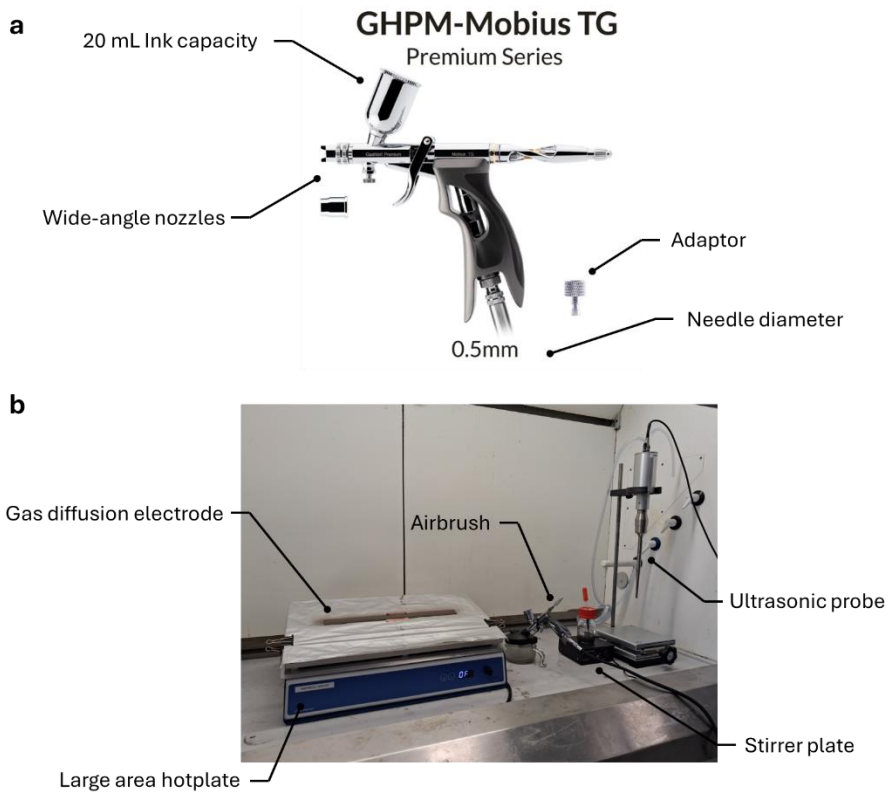

Fig. S 22 Experimental setup for spray-coating catalytic Ag-GDEs; (a) commercial Gaahleri airbrush used for spray-coating; (b) Photograph of the ink preparation and spray-coating setup assembled into a fume-cupboard.

GDLs of size 34 x 3 cm^2 typically gained a catalyst layer of ~130 mg in mass corresponding to a geometric loading of ~1.3 mg cm^{-2} and a catalyst loading of ~1.1 mg cm^{-2} (The ink mixture was assumed to be approximately 86 % wt. catalyst and 14 % wt. Nafion®). The airbrushing method was deliberately inefficient in terms of catalyst and Nafion® ink usage (20 % wt. utilised per GDE sample) to ensure homogenously coated electrodes. An apparent 80 % of the ink mixture was lost due to missing the

sample, being extracted by the fume-cupboard or coating the internal parts of the airbrush and glassware utilised. For transparency, catalyst loadings for each electrode prepared are provided in Table S 1.

Table S 1 Catalyst loadings for Ag-GDEs employed in this study for EC-CO2R and differential pressure measurements. Samples for threshold pressure measurements (TPM) and EC-CO2R electrolysis in a pumped electrode (PE) and falling-film electrode (FFE) experiments are presented.

GDE	Sample	Name	Cross-reference	Dimensions [cm^2]	Geometric area [cm^2]	Catalyst layer mass [mg]	Geometric loading [mg cm^{-2}]	Catalyst loading [mg cm^{-2}]
28BC-Ag	TPM	28BC-Ag-Square-1	Fig. 8	5 x 5	25	16.9	0.68	0.58
		28BC-Ag-Square-2	Fig. 8	5 x 5	25	28.1	1.12	0.96
		28BC-Ag-Square-3	Fig. 8	5 x 5	25	25.9	1.04	0.89
	FFE	28BC-Ag-Tall-1	Fig. S 32	34 x 3	102	65.2	0.64	0.55
		28BC-Ag-Tall-2	Fig. S 33	34 x 3	102	128.1	1.26	1.08
		28BC-Ag-Tall-3	Fig. S 34	34 x 3	102	129.8	1.27	1.09
		28BC-Ag-Tall-4	Fig. S 35	34 x 3	102	106	1.04	0.89
	PE	28BC-Ag-Tall-5	Fig. S 38	34 x 3	102	129.8	1.27	1.09
H15C13 -Ag	TPM	H15C13-Ag-Square-1	Fig. 8	5 x 5	25	38.9	1.56	1.33
		H15C13-Ag-Square-2	Fig. 8	5 x 5	25	31.6	1.26	1.08
		H15C13-Ag-Square-3	Fig. 8	5 x 5	25	41.2	1.65	1.41
	FFE	H15C13-Ag-Tall-1	Fig. 10	34 x 3	102	99.8	0.98	0.84
		H15C13-Ag-Tall-2	Fig. S 36	34 x 3	102	126.7	1.24	1.06
		H15C13-Ag-Tall-3	Fig. S 37	34 x 3	102	144.7	1.42	1.22
	PE	H15C13-Ag-Tall-4	Fig. S 39	34 x 3	102	218.3	2.14	1.83

Average	1.06
Uncertainty	0.32

Scanning electron microscopy

Scanning electron microscopy (SEM) was performed using a Hitachi TM3030Plus SEM at an acceleration voltage of 15 kV and a filament current of 1.85 A.

Sigracet 28BC GDL

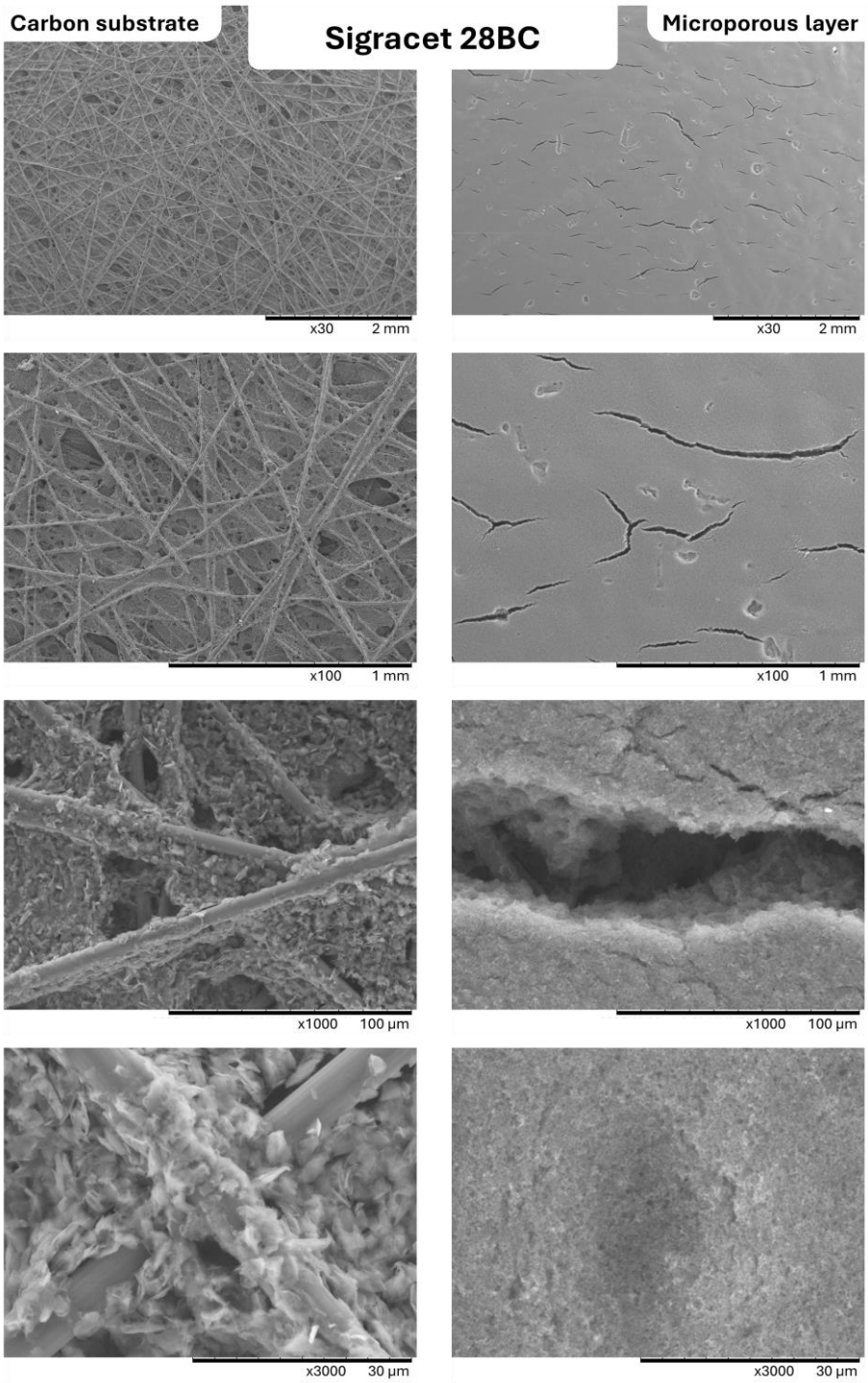

Fig. S 23 SEM images of pristine Sigracet 28BC GDL material at x30, x100, x1000 and x3000 magnifications. Images of the carbon substrate and microporous layer are provided.

Freudenberg H15C13 GDL

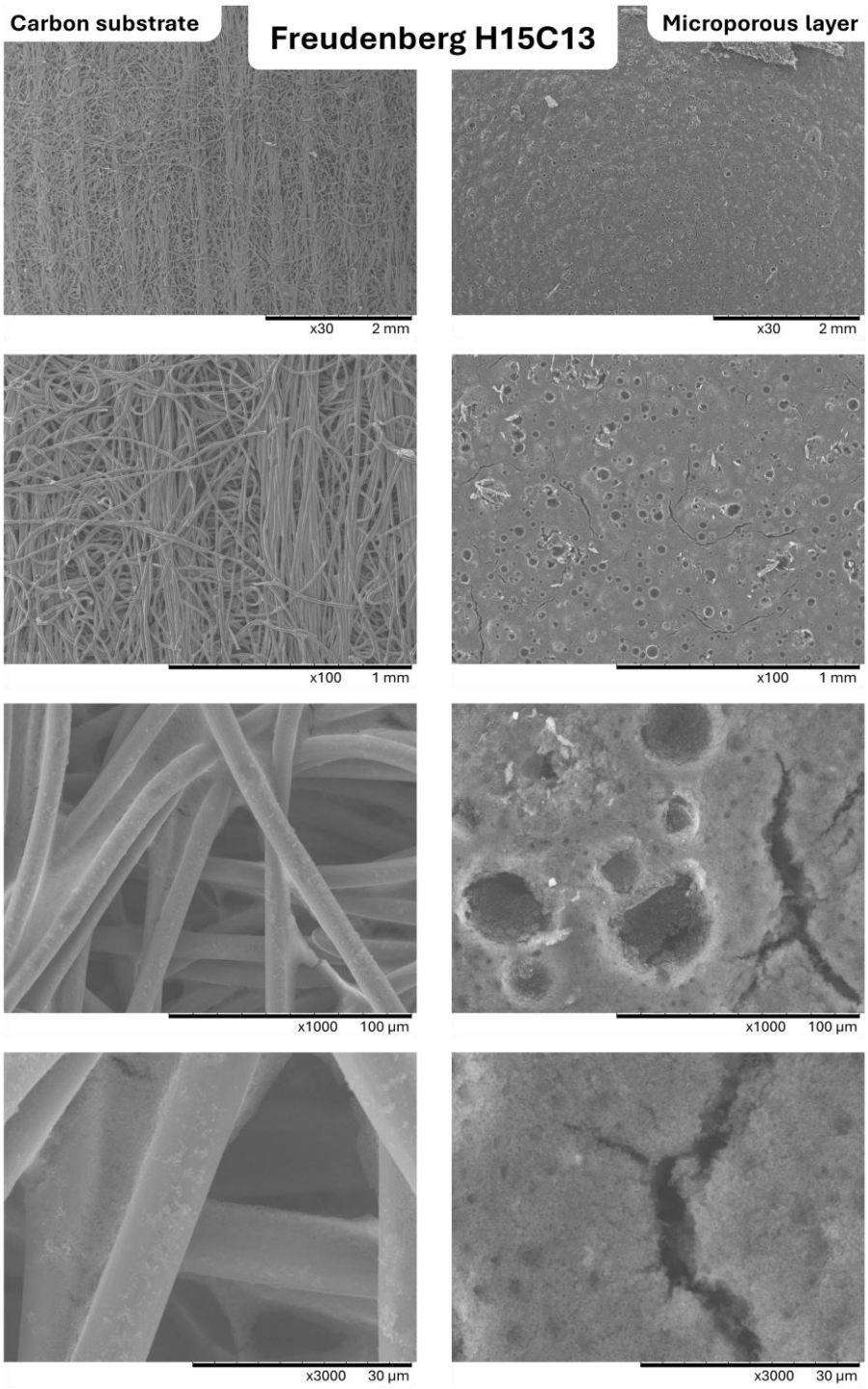

Fig. S 24 SEM images of pristine Freudenberg H15C13 GDL material at x30, x100, x1000 and x3000 magnifications. Images of the carbon substrate and microporous layer are provided.

Sigracet 28BC-Ag GDE

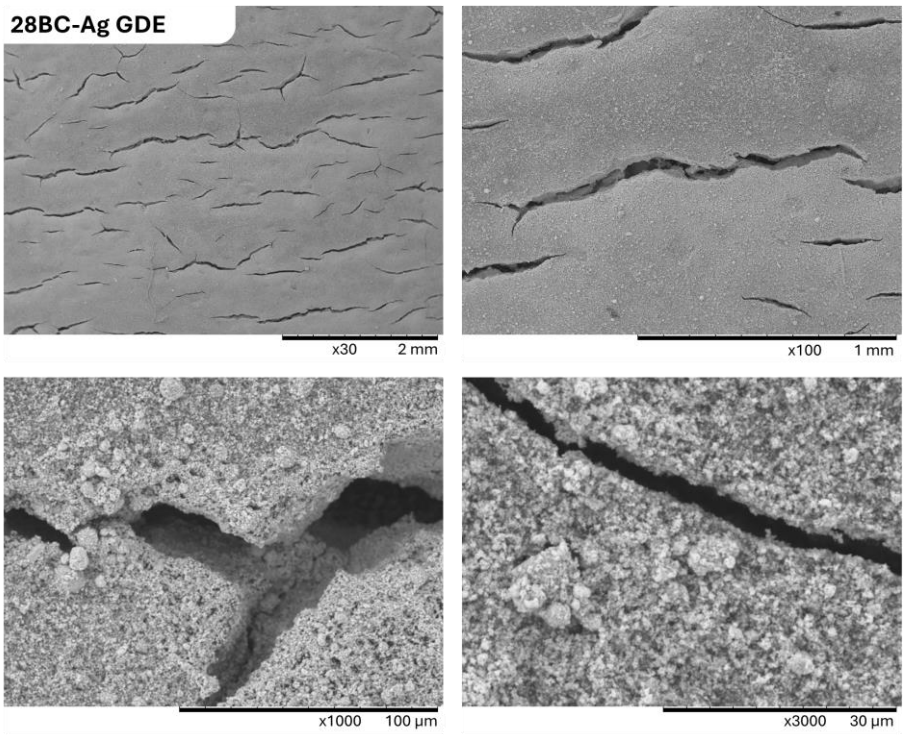

Fig. S 25 SEM images of Sigracet 28BC-Ag GDE catalyst layer at x30, x100, x1000 and x3000 magnifications.

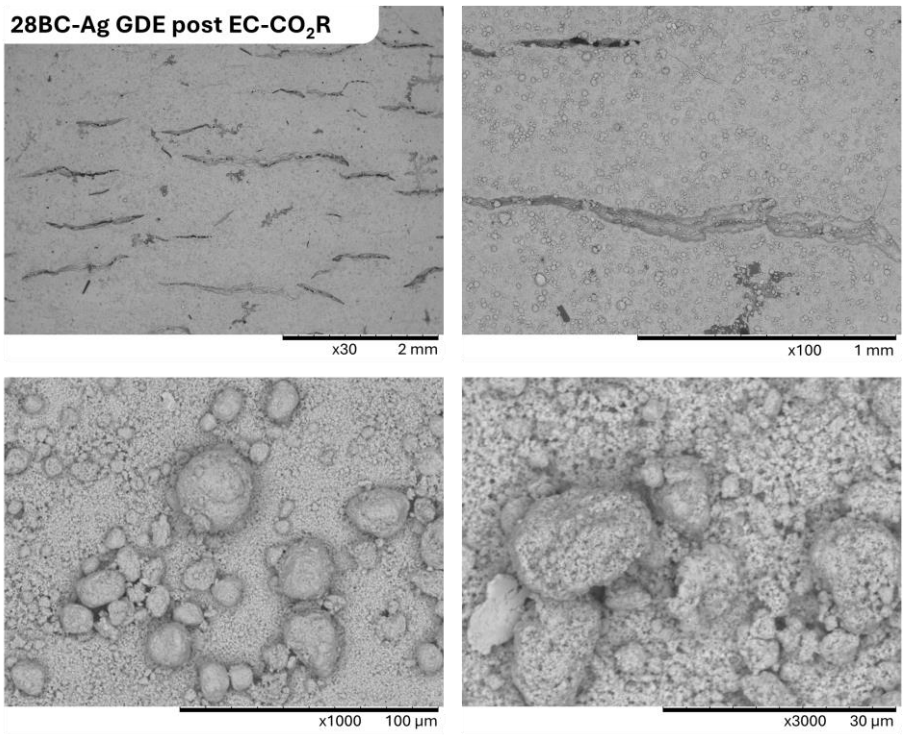

Fig. S 26 SEM images of Sigracet 28BC-Ag GDE catalyst layer after 8 h of EC-CO_2R at x30, x100, x1000 and x3000 magnifications. Residual $KHCO_3$ electrolyte crystals were visible on the catalyst layer despite rinsing with ultrapure water.

Freudenberg H15C13-Ag GDE

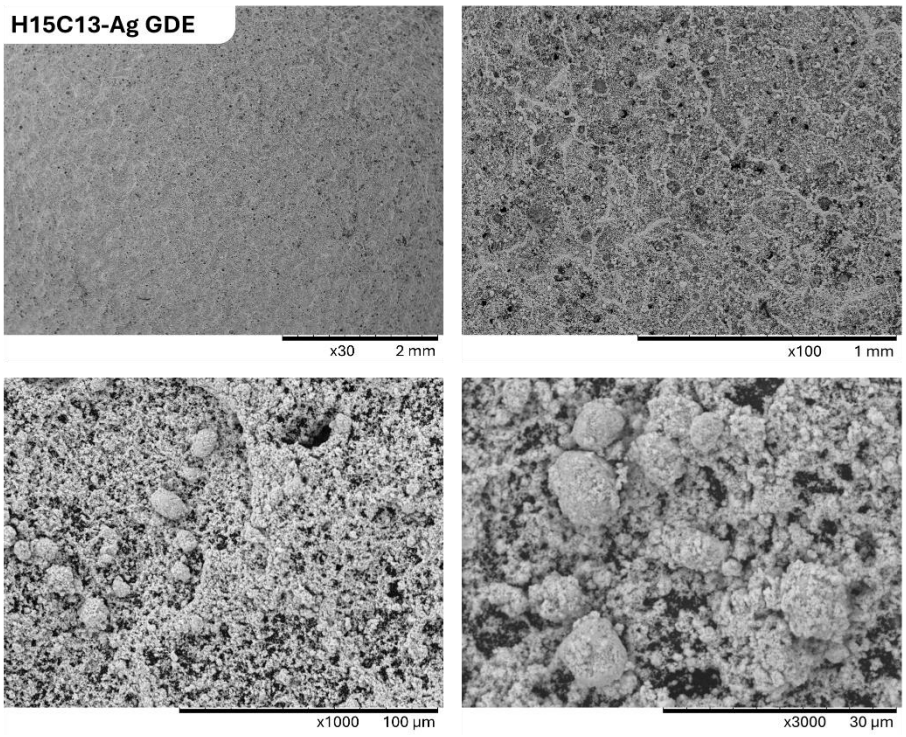

Fig. S 27 SEM images of Freudenberg H15C13-Ag GDE catalyst layer at x30, x100, x1000 and x3000 magnifications.

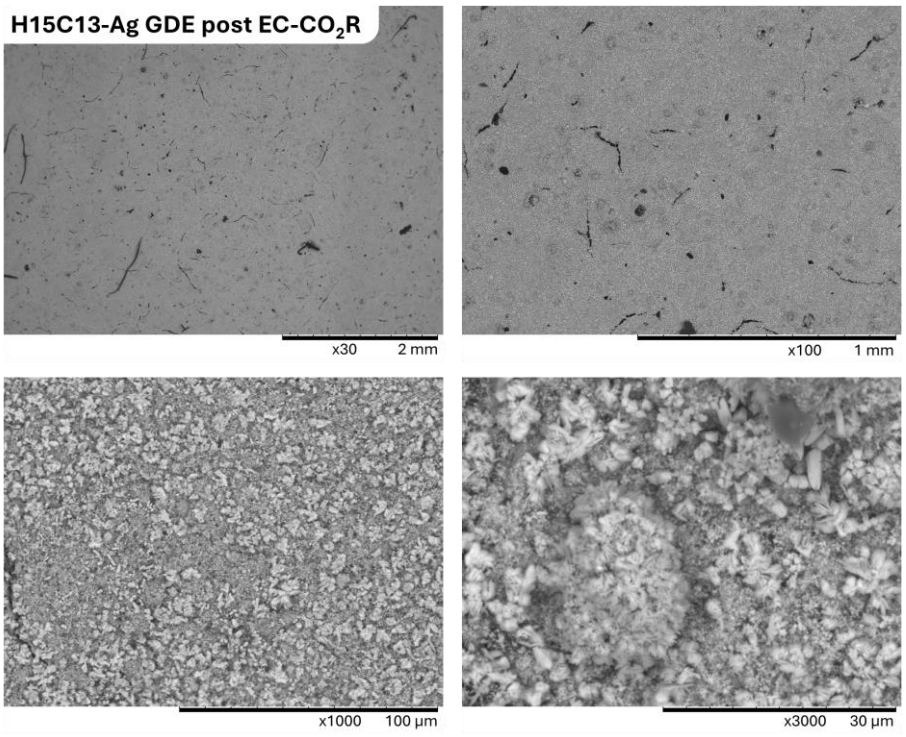

Fig. S 28 SEM images of Freudenberg H15C13-Ag GDE catalyst layer after 8 h of EC-CO_2R at x30, x100, x1000 and x3000 magnifications. Residual $KHCO_3$ electrolyte crystals were visible on the catalyst layer despite rinsing with ultrapure water.

Water contact angle

Water contact angles for quantifying hydrophobicity were measured using a Krüss Drop Shape Analyser instrument and 4 µL droplet volume of ultrapure water. For each material type, 3 samples were examined, and 5 droplets were recorded for each sample giving an averaged result over 15 droplets. Contact angles for each material type of pristine and unused 28BC, H15C13, 28BC-Ag and H15C13-Ag are provided, in addition to comparable 28BC-Ag and H15C13-Ag samples post EC-CO_2R electrolysis. Post electrolysis samples were rinsed with ultrapure water and thoroughly dried under vacuum before analysis. This caused a noteworthy recovery of the GDE hydrophobicity because samples were fully wetted upon cell disassembly and their water contact angle could not be measured in this condition. Electrolyte crystal growths were observed on both sides of the GDE upon vacuum drying, highlighting the full ingress of electrolyte through the GDE layers.

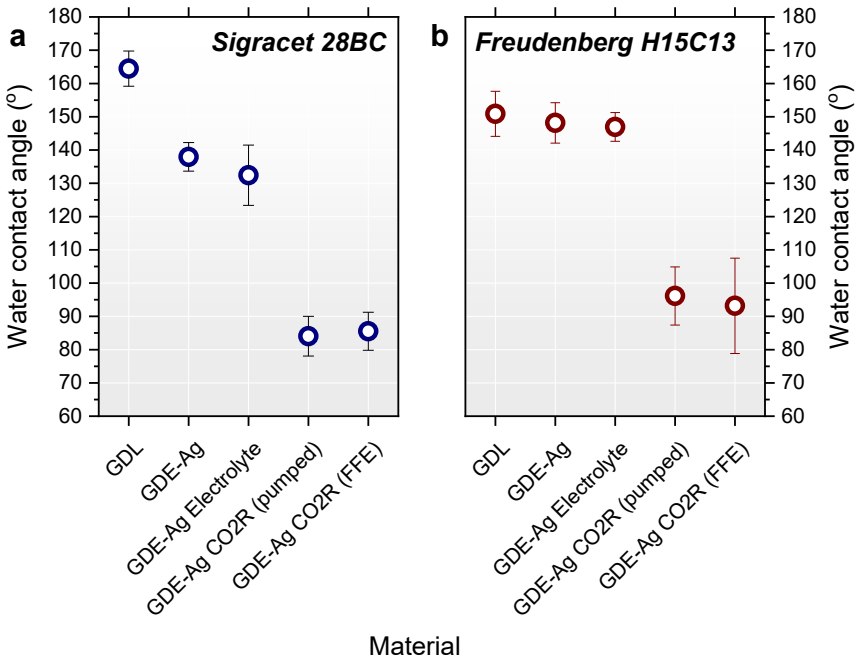

Fig. S 29 Water contact angle measurements for (a) 28BC and (b) H15C13 GDL materials and corresponding Ag-GDEs. Freshly prepared Ag-GDEs are compared to Ag-GDEs which were exposed to 1 M $KHCO_3$ for 1 h, and to Ag-GDEs which were used in 8 h electrolysis experiments with either a FFE or pumped recirculation method.

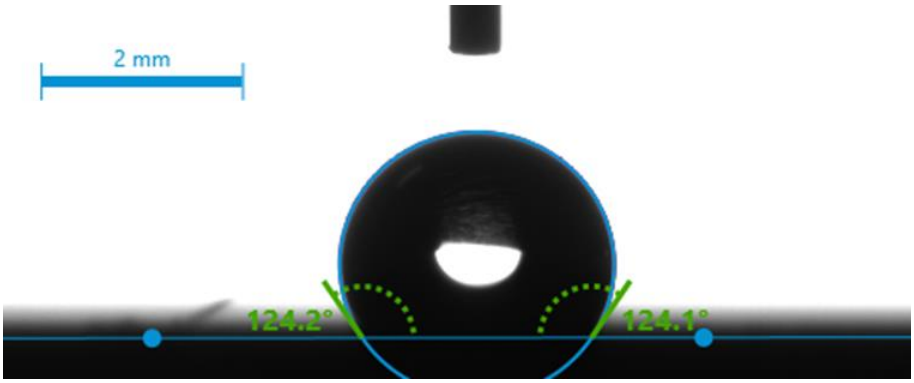

Fig. S 30 Water contact angle determination for 28BC.

Electrochemistry

Electrochemical impedance spectroscopy

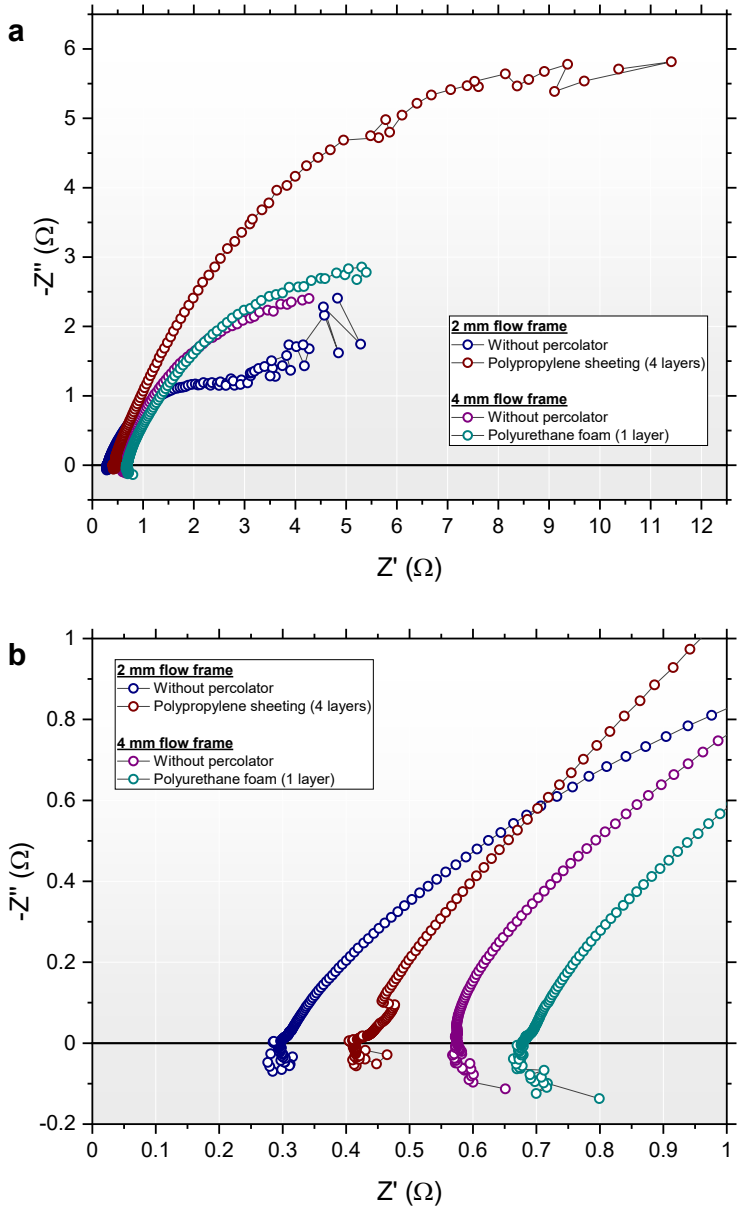

Fig. S 31 EIS analysis of the 32 x 1 cm² FFE with and without percolators. The full data range is shown in (a), and high frequency intercepts are shown in (b). In each case a fresh 28BC-Ag GDE is tested with static electrolyte.

Electrolysis: galvanostatic with falling film electrolyte

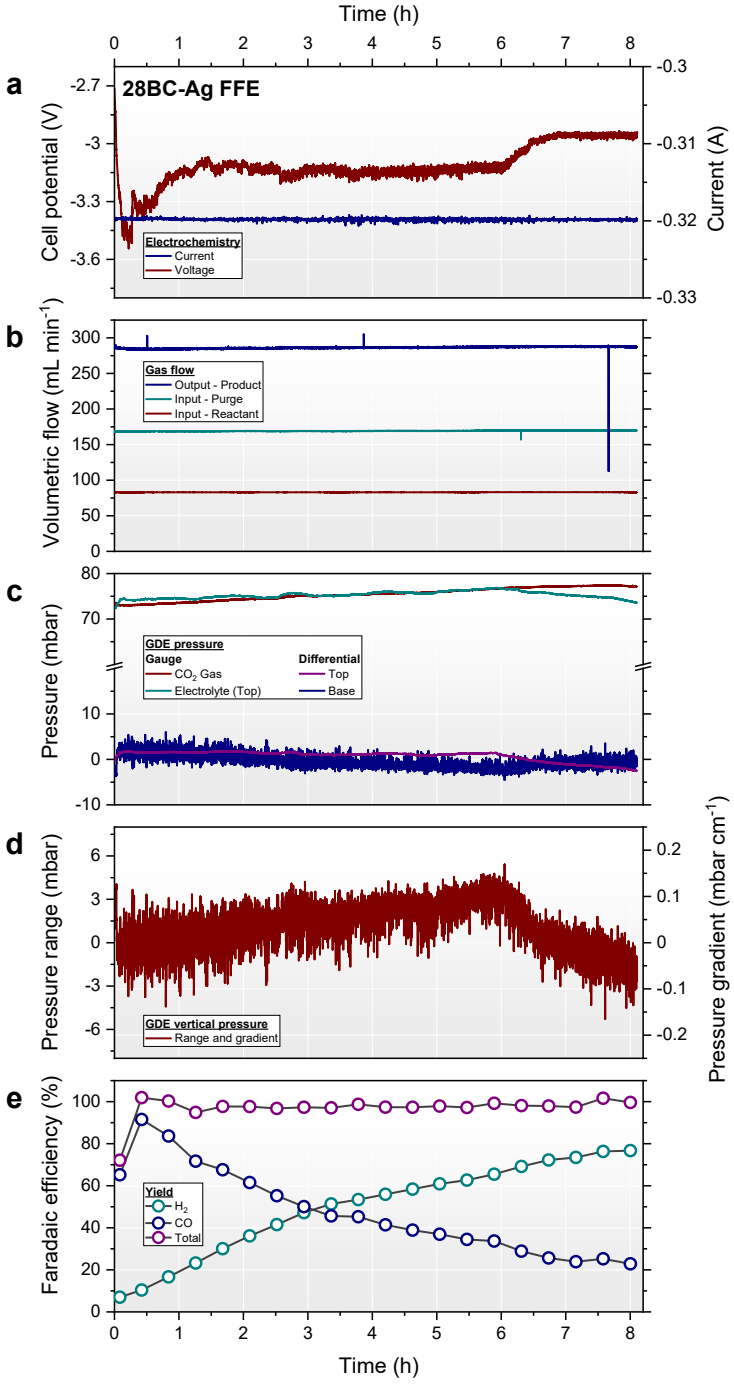

Fig. S 32 EC-CO_2R at a vertically pressure balanced 28BC-Ag GDE with a gravity-driven catholyte, using a polyurethane foam percolator. The (a) cell potential, (b) electrolyser CO_2 flow rates, (c) GDE pressures, (d) vertical GDE pressure range and gradient, and (e) electrolyser yields are presented.

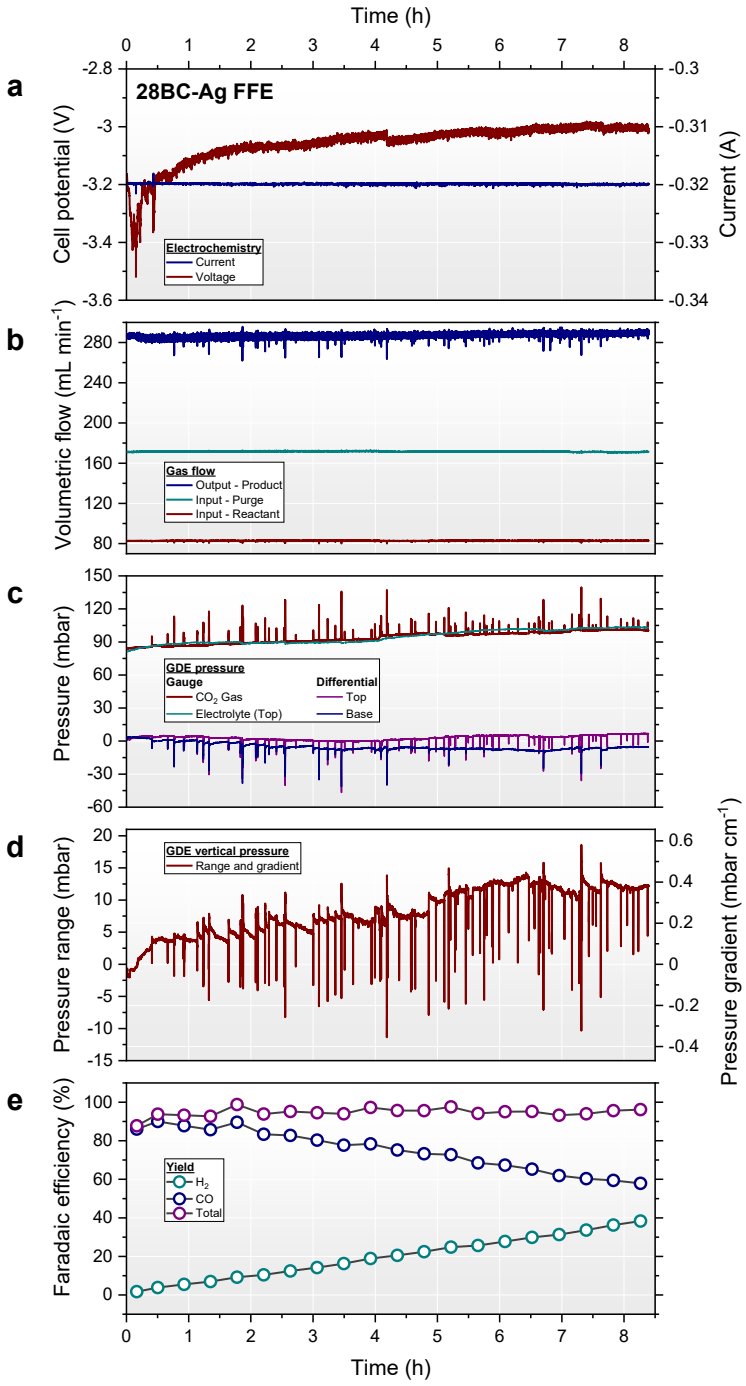

Fig. S 33 EC-CO_2R at a vertically pressure balanced 28BC-Ag GDE with a gravity-driven catholyte, using a polyurethane foam percolator. The (a) cell potential, (b) electrolyser CO_2 flow rates, (c) GDE pressures, (d) vertical GDE pressure range and gradient, and (e) electrolyser yields are presented.

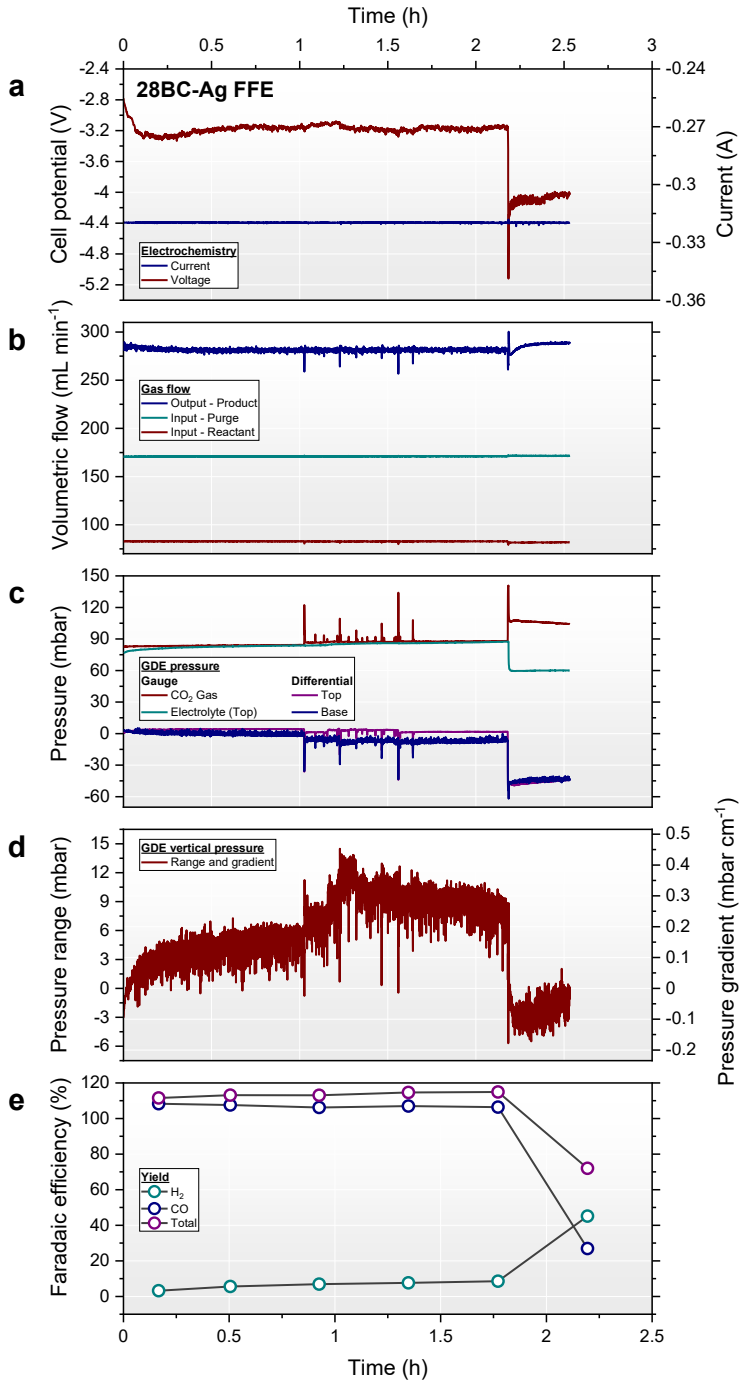

Fig. S 34 EC-CO_2R at a vertically pressure balanced 28BC-Ag GDE with a gravity-driven catholyte, using a polyurethane foam percolator. The (a) cell potential, (b) electrolyser CO_2 flow rates, (c) GDE pressures, (d) vertical GDE pressure range and gradient, and (e) electrolyser yields are presented. Excessive electrolyte flooding caused the GDE to fail due to the blockage of electrolyte flow via gas breakthrough as described in the manuscript.

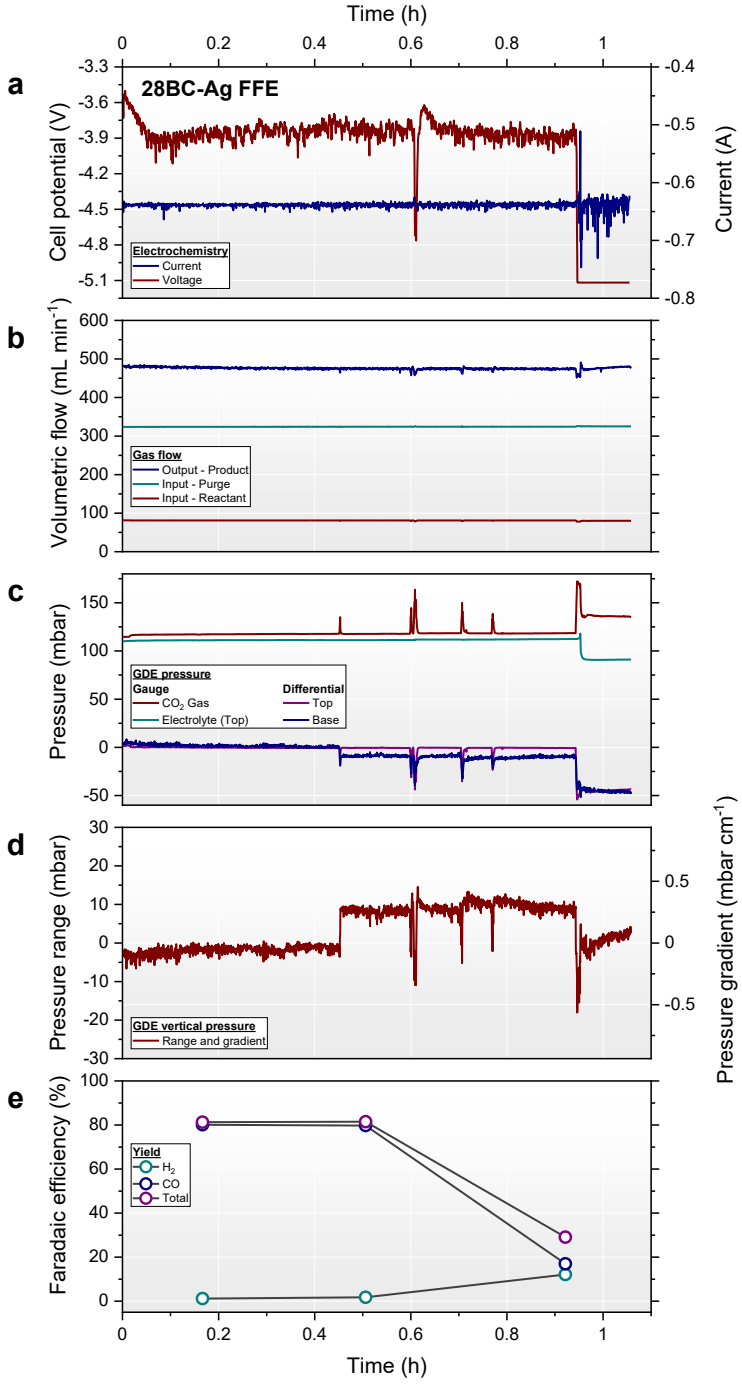

Fig. S 35 EC-CO_2R at a vertically pressure balanced 28BC-Ag GDE with a gravity-driven catholyte, using a polyurethane foam percolator. The (a) cell potential, (b) electrolyser CO_2 flow rates, (c) GDE pressures, (d) vertical GDE pressure range and gradient, and (e) electrolyser yields are presented. Excessive electrolyte flooding caused the GDE to fail due to the blockage of electrolyte flow via gas breakthrough as described in the manuscript.

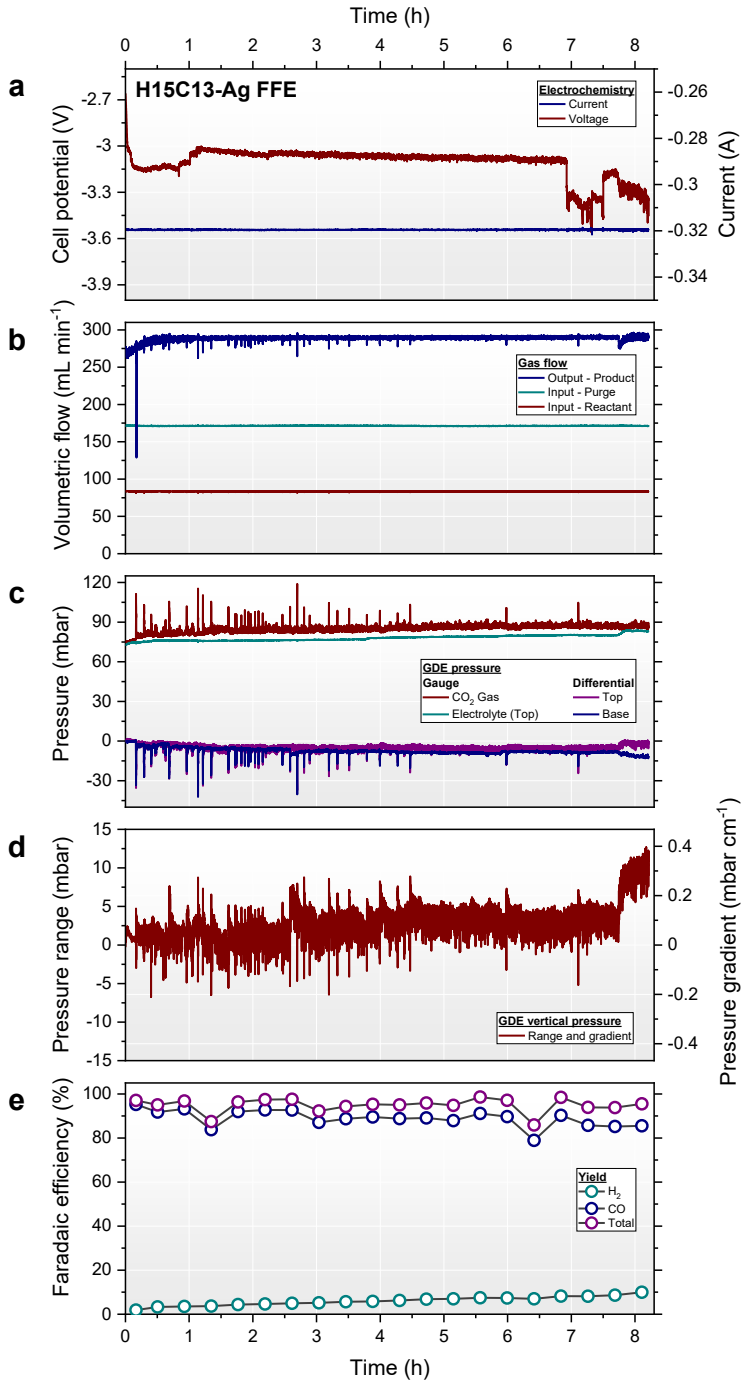

Fig. S 36 EC-CO2R at a vertically pressure balanced H15C13-Ag GDE with a gravity-driven catholyte, using a polyurethane foam percolator. The (a) cell potential, (b) electrolyser CO_2 flow rates, (c) GDE pressures, (d) vertical GDE pressure range and gradient, and (e) electrolyser yields are presented. This is a repetition of the H15C13-Ag experiment given in the manuscript.

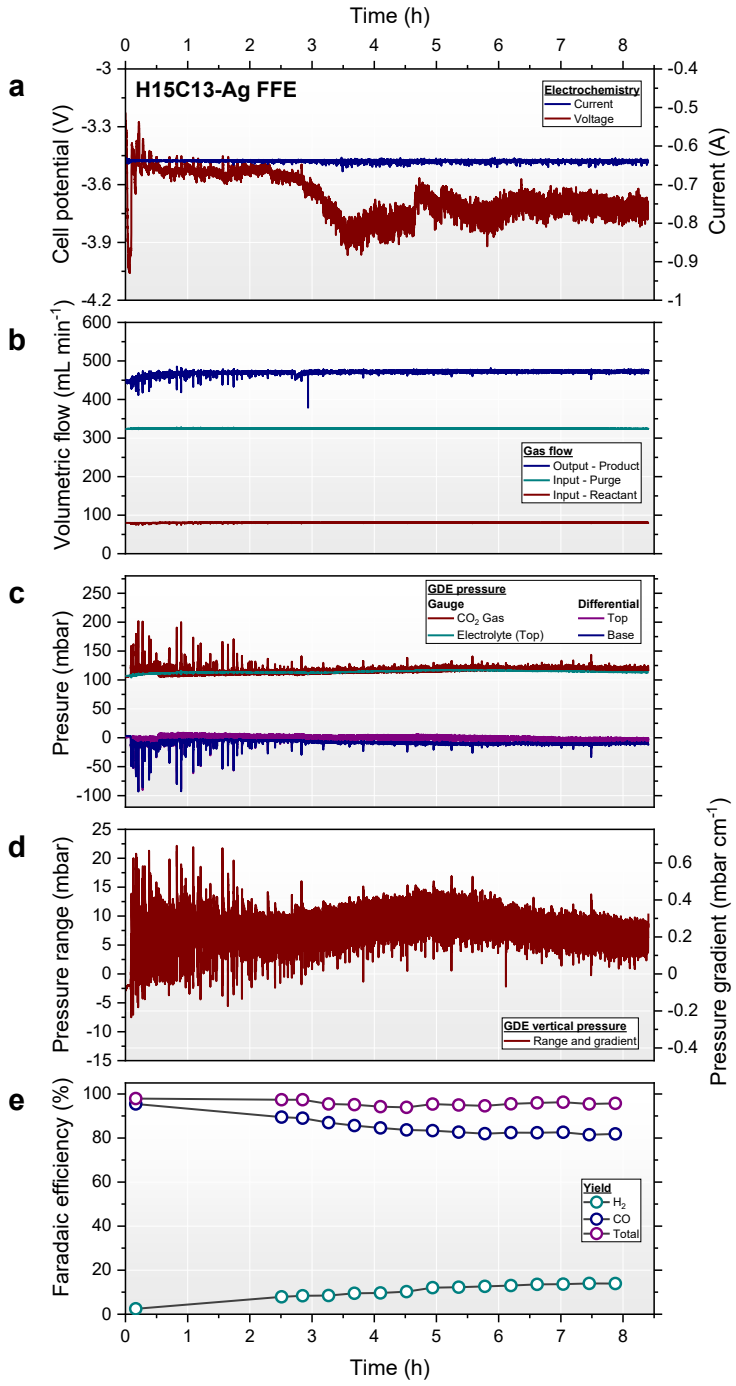

Fig. S 37 EC-CO_2R at a vertically pressure balanced H15C13-Ag GDE with a gravity-driven catholyte, using a polyurethane foam percolator. The (a) cell potential, (b) electrolyser CO_2 flow rates, (c) GDE pressures, (d) vertical GDE pressure range and gradient, and (e) electrolyser yields are presented. This is a repetition of the H15C13-Ag experiment given in the manuscript, but at 20 mA cm^{-2} current density. Missing yield data between 10 and 150 min was due to an unexpected gas chromatography fault.

Electrolysis: galvanostatic with pumped electrolyte

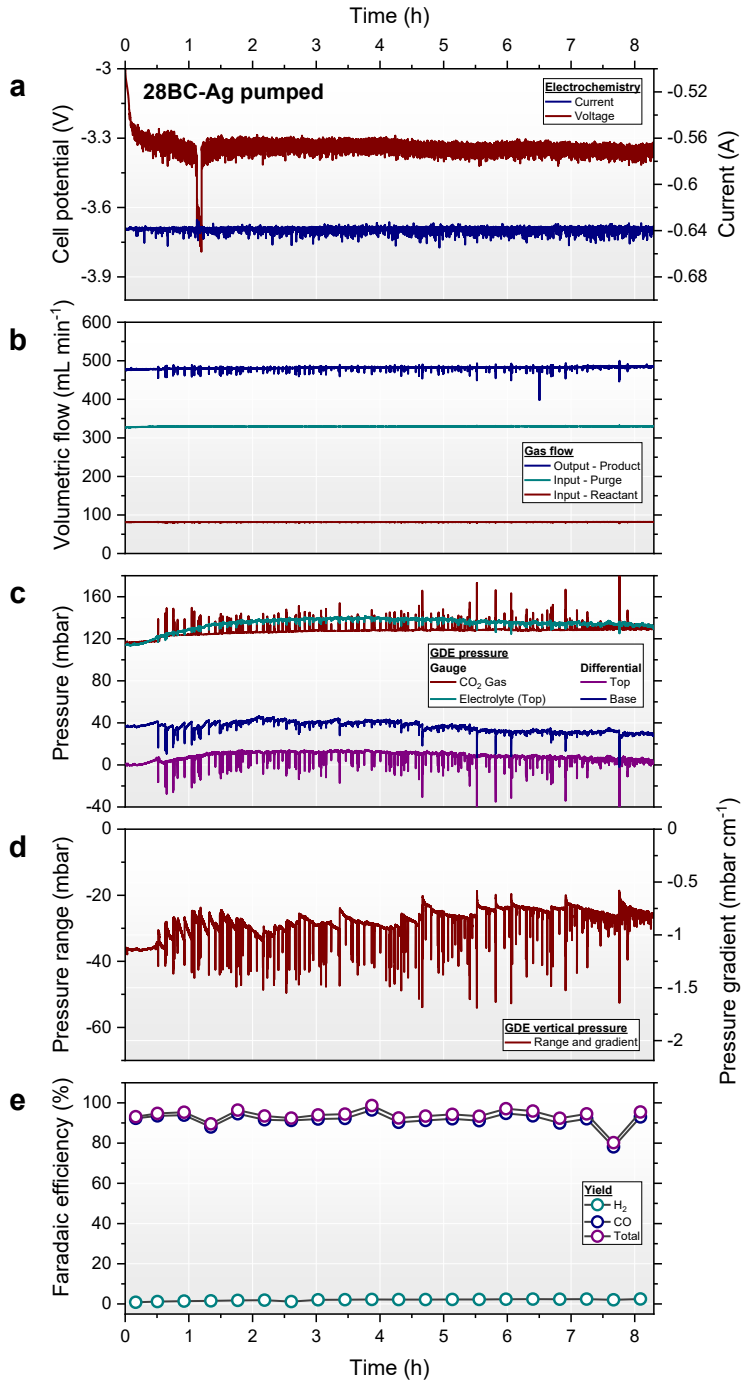

Fig. S 38 EC-CO2R at a 28BC-Ag GDE with an upwards pumped catholyte at 165 mL min-1 without a percolator. The (a) cell potential, (b) electrolyser CO2 flow rates, (c) GDE pressures, (d) vertical GDE pressure range and gradient, and (e) electrolyser yields are presented. 20 mA cm-2 current density.

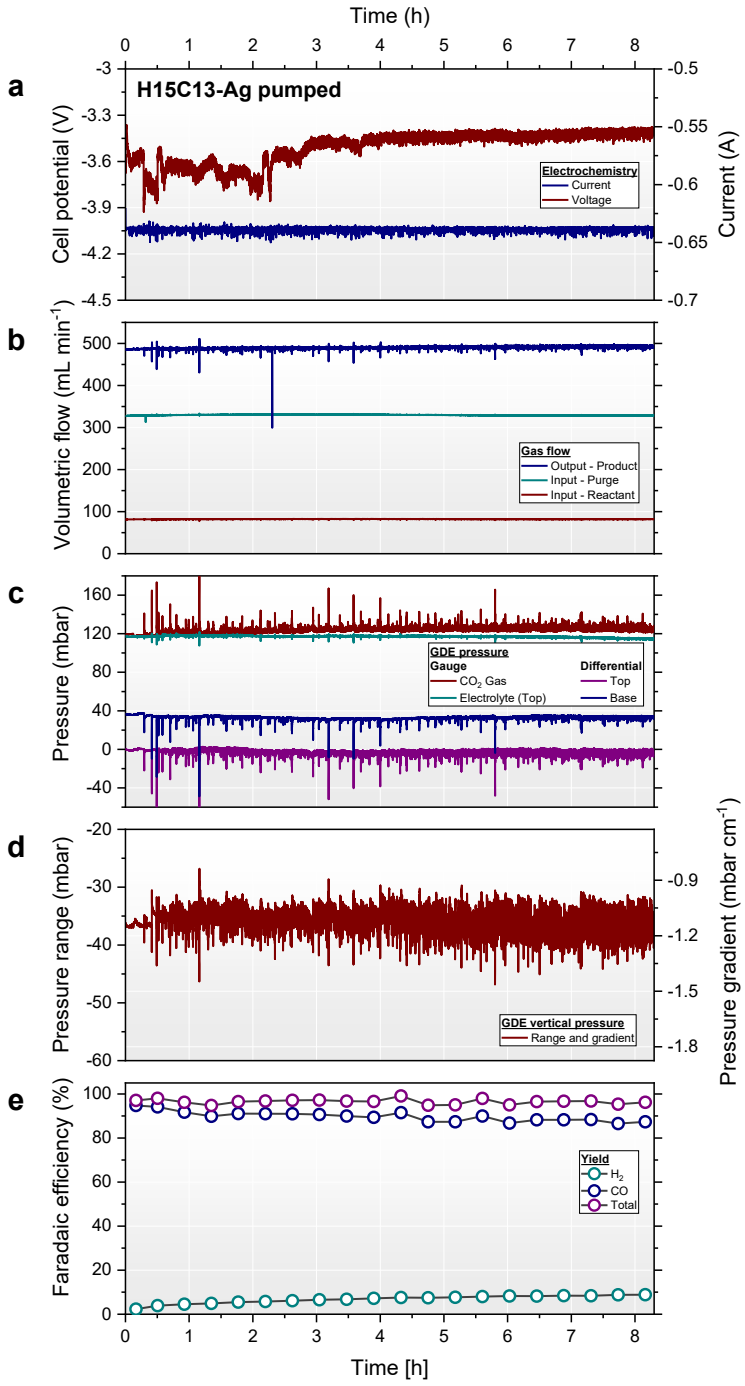

Fig. S 39 EC-CO_2R at a H15C13-Ag GDE with an upwards pumped catholyte at 165 mL min^{-1} without a percolator. The (a) cell potential, (b) electrolyser CO_2 flow rates, (c) GDE pressures, (d) vertical GDE pressure range and gradient, and (e) electrolyser yields are presented. 20 mA cm^{-2} current density.

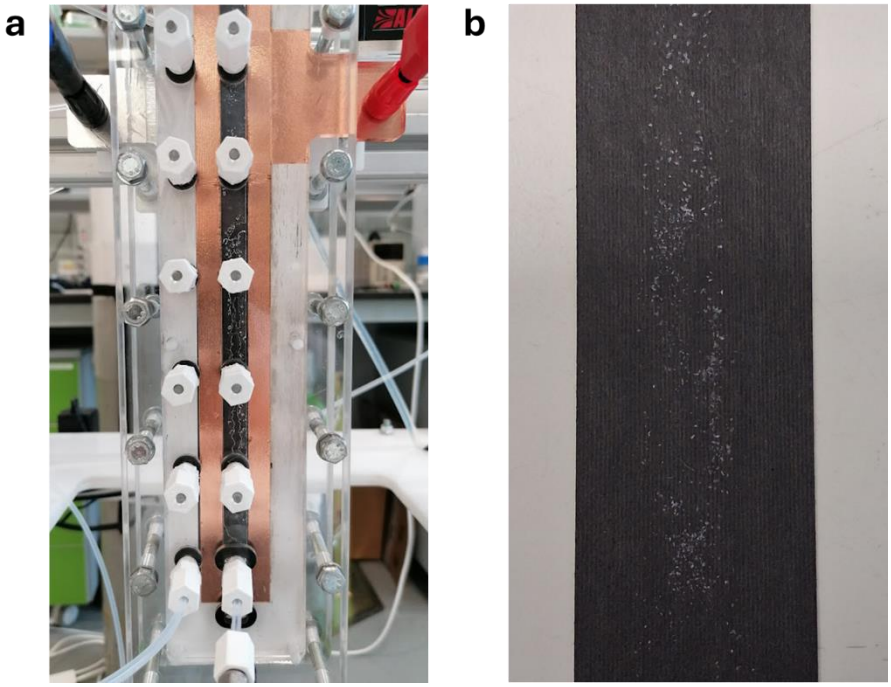

Fig. S 40 Visual observations of H15C13-Ag GDE flooding resulting from electrolysis experiments; (a) Droplets of electrolyte emerging from the GDE CS and pooling within the CO_2 chamber were visible during electrolysis; (b) The crystallisation of $KHCO_3$ electrolyte on the reverse side (CS) of the GDE in central areas exposed to electrolyte was visible after drying.

Gas chromatograph calibration

The Agilent 7820A GC employed was pre-calibrated for H_2, CO, CH_4, C_2H_4 and C_2H_6 within the range of ≈100 to 10,000 ppm by dilutions of bespoke 1 and 0.1 % calibration gasses supplied by British Oxygen Company Ltd. (*i.e.* the 1 % cylinder contained 1 % H_2, 1 % CO, 1 % CH_4, 1 % C_2H_4 and 1 % C_2H_6). The dilutions were prepared by use of a custom-designed pressure vessel constructed from Swagelok fittings, shown schematically in Fig. S 41. Samples were prepared by firstly evacuating the vessel of air under vacuum (to -1 bar), and then filling the vessel with $P_{\text{Calibration Gas}}$ and then P_{Nitrogen} such that $P_{\text{Total}} = P_{\text{Calibration Gas}} + P_{\text{Nitrogen}}$. Here, pressures are absolute pressures and P_{Total} was typically +2 bar. The resulting sample concentration was then calculated from:

$$C_{\text{Sample}} = \frac{P_{\text{Calibration Gas}}}{P_{\text{Calibration gas}} + P_{\text{Nitrogen}}} C_{\text{Calibration Gas}}$$

The calibration curves for the calibrated analytes are shown in Fig. S 42.

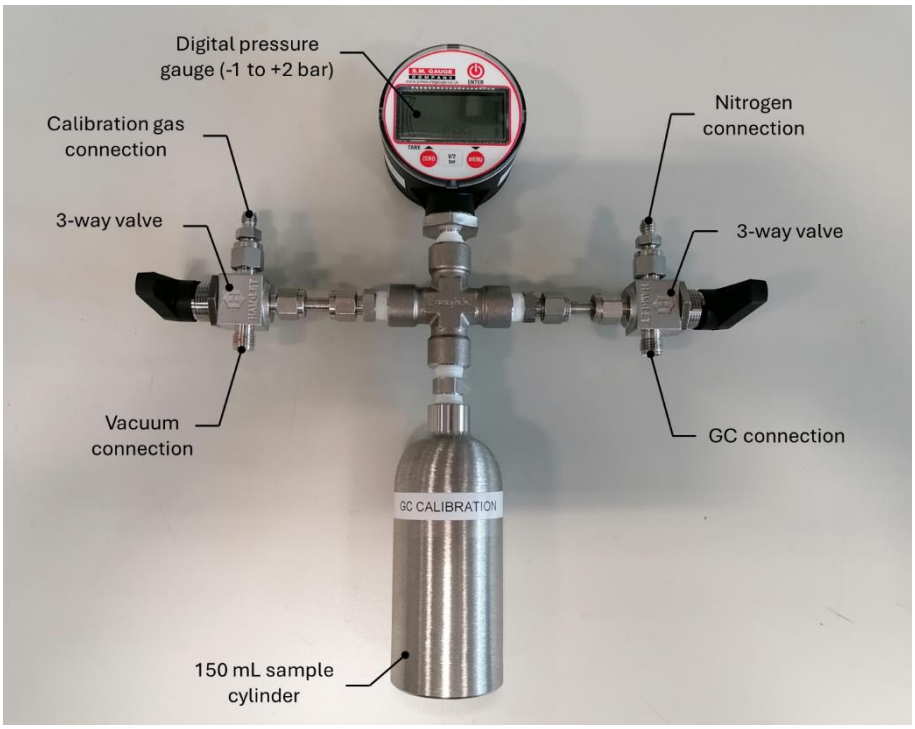

Fig. S 41 Schematic photograph of the pressure vessel employed for calibration of the GC instrument. The gas and vacuum connections are annotated.

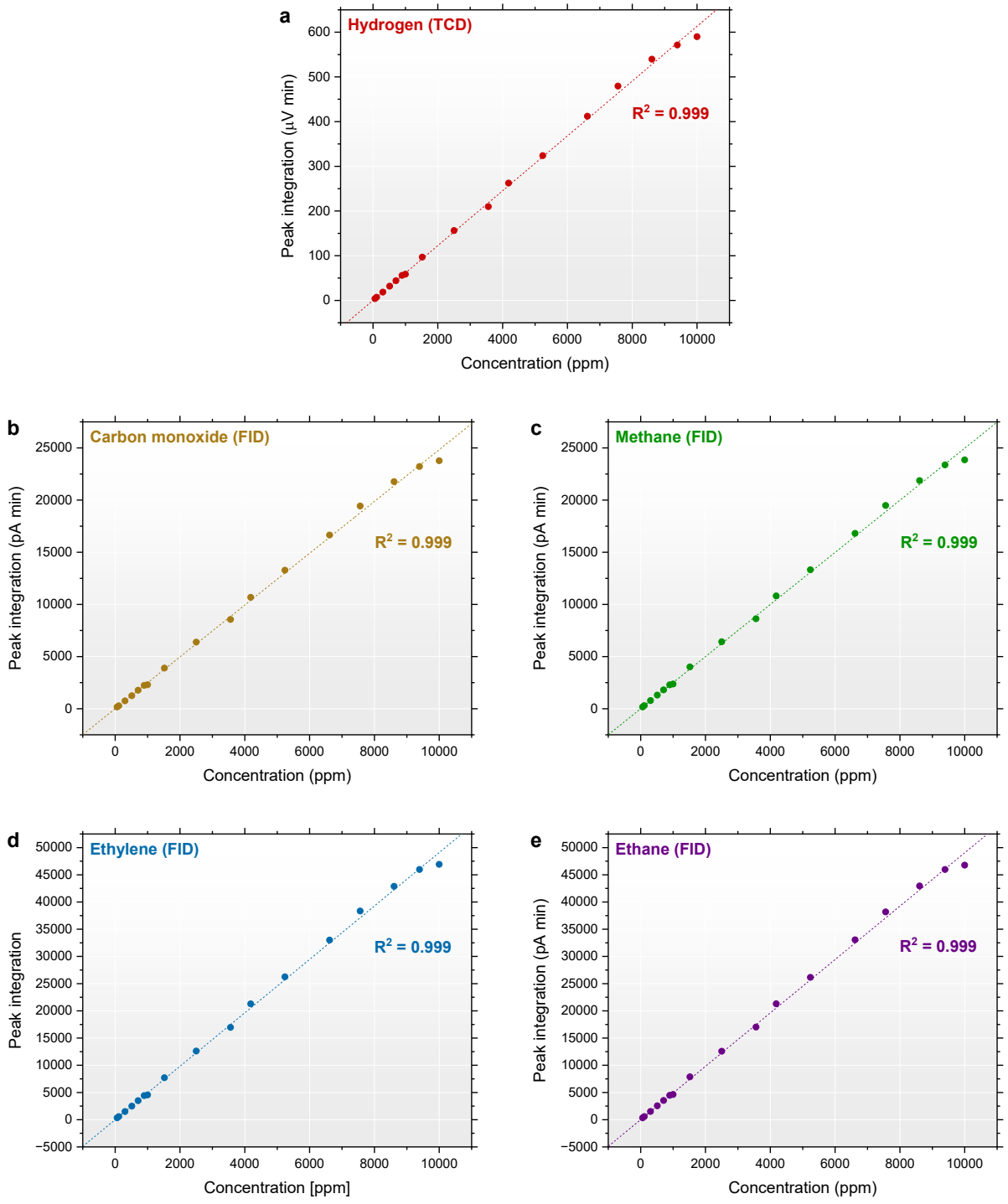

Fig. S 42 GC calibration curves for (a) H_2, (b) CO, (c) CH_4, (d) C_2H_4 and (e) C_2H_6. It should be noted that all calibration curves and associated R^2 values are related because the calibration gas contained all five analytes, thus making all dilutions self-consistent.

Manuscript glossary

Abbreviations

28BC-Ag/28BC	SGL Carbon Sigracet 28BC gas diffusion layer with/without silver catalyst layer
CL	Catalyst layer
CS	Carbon substrate
EC-CO_2R	Electrochemical carbon dioxide reduction
EF	Electrolyte flooding
EIS	Electrochemical impedance spectroscopy
ESI	Electronic supporting information
FFE	Falling film electrolyser
GBT	Gas breakthrough
GC	Gas chromatograph
GDE	Gas diffusion electrode
GDL	Gas diffusion layer
H15C13-Ag/ H15C13	Freudenberg H15C13 gas diffusion layer with/without silver catalyst layer
HER	Hydrogen evolution reaction
H-S	Hele-Shaw (cell)
mbarD	Differential pressure in units of mbar
MPL	Microporous layer
ODC	Oxygen depolarised cathode
OER	Oxygen evolution reaction
PP	Polypropylene
PTFE	Polytetrafluoroethylene
PU	Polyurethane
PPI	Pores per inch
SEM	Scanning electron microscopy

Symbols

A	Area
θ	Contact angle
ρ	Density
s	Distance from percolator inlet
z	Elevation
z_b, z_d, z_f, z_t	Elevation, percolator base, drain reservoir, feed reservoir and percolator top
Q	Flow rate
Q_c	Flow rate, critical
q	Flux
g	Gravitational acceleration
K	Hydraulic conductivity
h	Hydraulic head
h_b, h_d, h_f, h_t	Hydraulic head, percolator base, drain reservoir, feed reservoir and percolator top
Δh	Hydraulic head, difference
γ	Interfacial surface tension
L	Length, percolator
k	Permeability
k_eff	Permeability, effective
P	Pressure
P_b, P_d, P_f, P_t	Pressure, percolator base, drain reservoir, feed reservoir and percolator top
P_c, P_g, P_l	Pressure, capillary, gas and liquid
P_0	Pressure, ambient
ΔP	Pressure, differential
δP	Pressure, differential range
r	Radii
Δz_Res	Reservoir elevation difference
ν	Velocity
μ	Viscosity